Higgs CP studies at ATLAS+CMS

9th Large Hadron Collider Physics (LHCP2021)

María Moreno Llácer (IFIC, CSIC-Uni. Valencia),
on behalf of ATLAS and CMS Collaborations

Zoom meeting

Testing the CP nature of the Higgs boson

Understanding the CP property of the Higgs boson is one of the most important topics in particle physics today.

In the Standard Model:

- the only source of CP violation comes from CKM phase
- the Higgs boson has scalar (CP-even) couplings to SM particles

→ Need to test these since any CP-odd contribution would be a sign of BSM!

Probing couplings to bosons (HVV and Hgg):

- decay channels with clean signature ($H \to ZZ^* \to 4l$, $H \to WW^* \to e\nu\mu\nu$) allow to study ggH production mode
- using VBF production: $H \to \tau\tau$ is essential due to its high BR
- using $H \to VV$ decay: $H \to ZZ^* \to 4l$ is the most sensitive channel due to its clean signature and absence of missing neutrinos

to fermions (Hff):

- Htt: using ttH production to probe top Yukawa
- $H\tau\tau$: recently studied in $H \to \tau\tau$ decay

CP-odd contributions in HVV couplings (from dim-6 operators) are suppressed with a $1/\Lambda^2$.

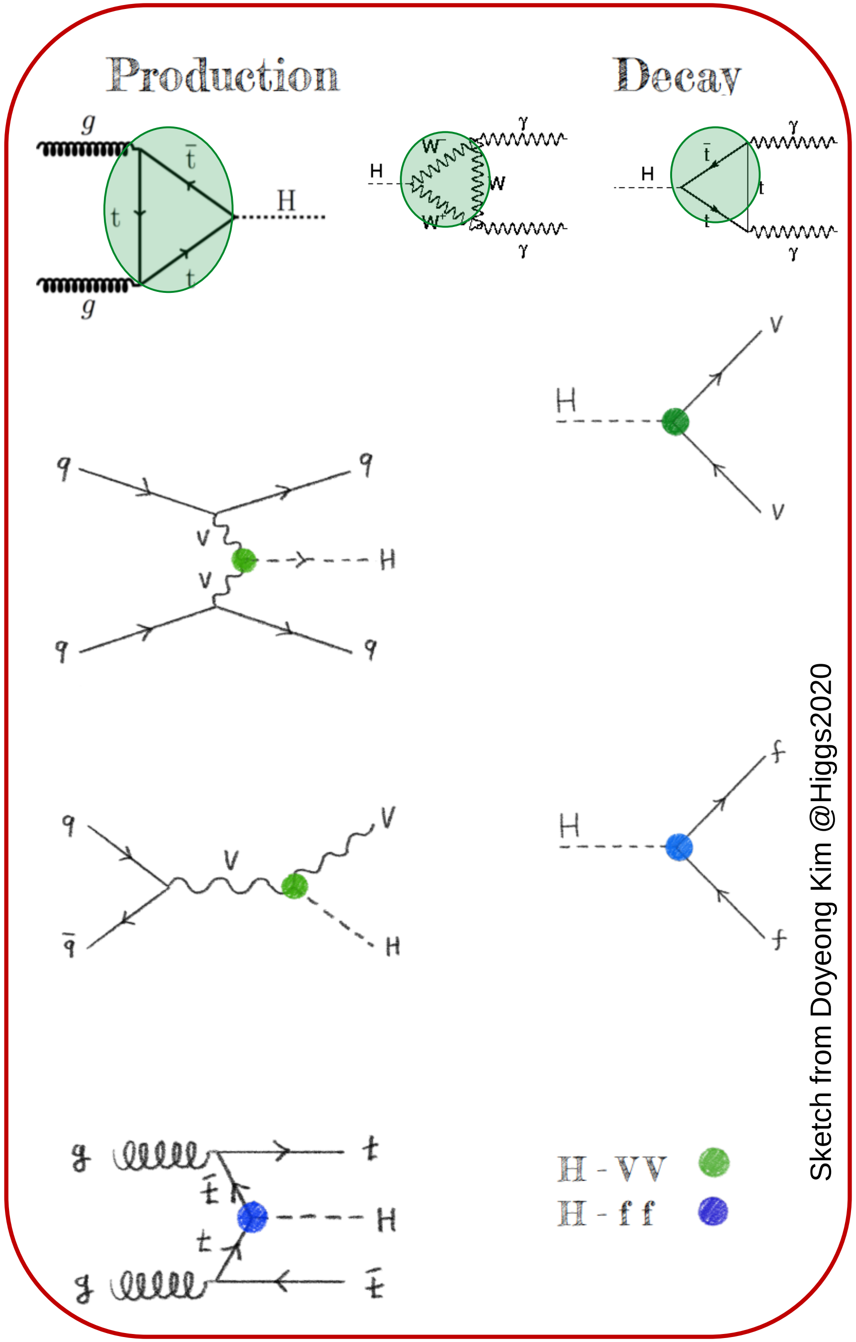

LHC Run2 results testing the CP nature of the Higgs boson

Direct searches	ATLAS	CMS
H→4l *(all prod. modes: H+2j, VH, ttH)*	{HVV, Hgg, Htt} EFT coefficients (Warsaw basis) *reinterpretation of cross-section measurements** EPJC(2020)80:957, full Run2	HVV, Hgg, Htt anomalous couplings & EFT coefficients (Higgs and Warsaw basis) using MELA disc. NEW **arXiv:2104.12152** (sub. to PRD), full Run2
H→WW*→eνμν *(prod. mode: H+2j)*	Hgg NEW anomalous couplings HC model (mass basis), using signed $\Delta\phi_{jj}$ **ATLAS-CONF-2020-055**, 36 fb^{-1}	---
H→ττ	HVV anomalous couplings using $O_{optimal}$ (CP-odd only, targets VBF) PLB805 (2020)135426, 36 fb^{-1} Hττ ATL-PHYS-PUB-2019-008, HL-LHC prospects	HVV anomalous couplings using MELA disc. PRD100,112002(2019), 36 fb^{-1} NEW Hττ $\|\phi\|$<36º @95%CL, using ϕ_{CP} , VBF+ggH+VH Pure CP-odd coupling excluded > 3σ **CMS-PAS-HIG-20-006**, full Run2
ttH (H→γγ)	Htt Higgs Charact. model, $\|\phi\|$<43º @95%CL Pure CP-odd coupling excluded > 3σ PRL125,061802(2020), full Run2	Htt using MELA disc., $\|\phi\|$<55º @95%CL Pure CP-odd coupling excluded > 3σ PRL125,061801(2020), full Run2

*ATLAS-CONF-2019-029: interpretations in H→γγ decay mode

→ This talk will focus on the **new results** (since LHCP2020)

Probing Hττ coupling structure

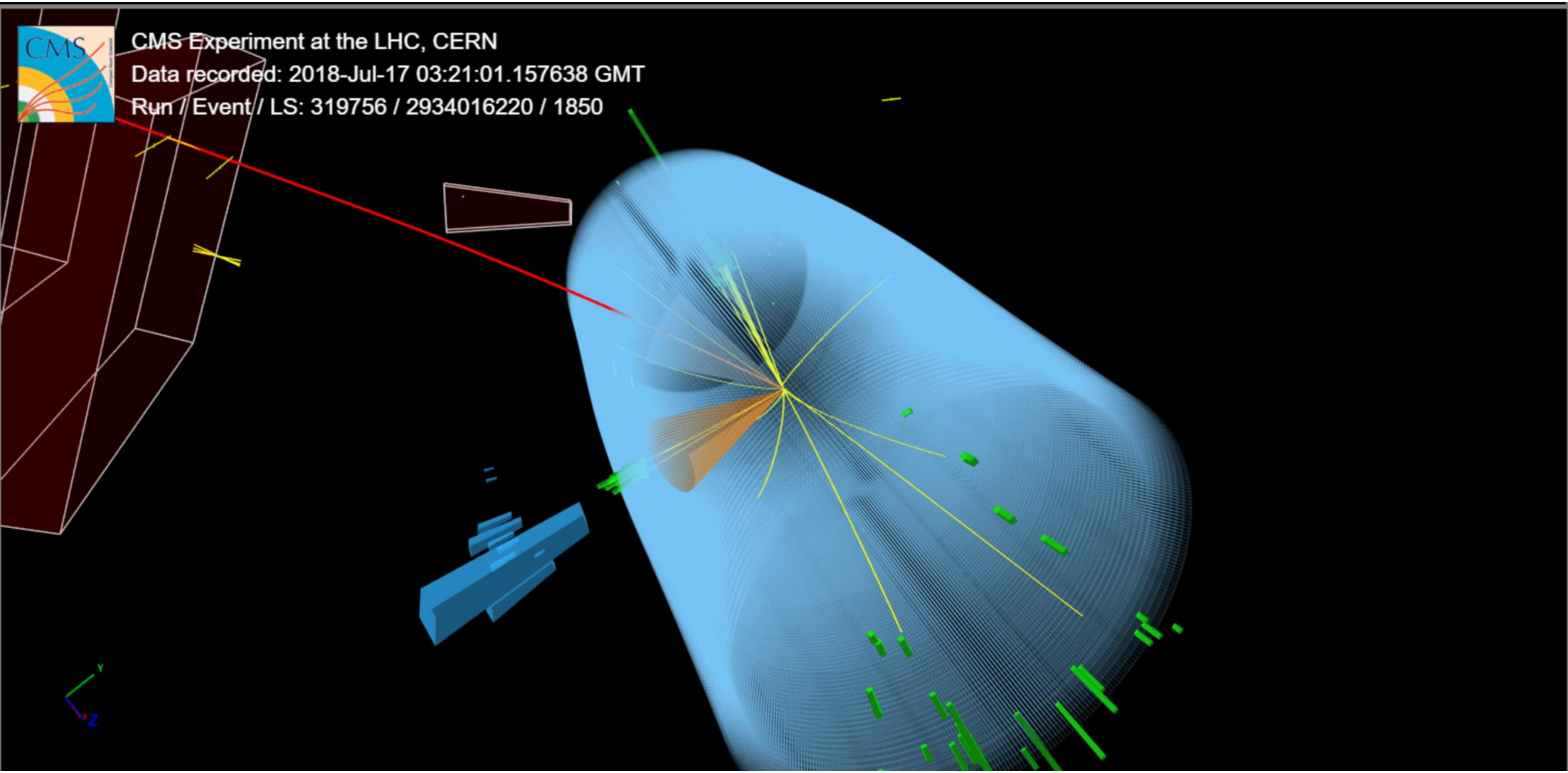

Probing Higgs-fermion interactions

Parametrise Higgs fermionic couplings in the mass eigenstate basis:

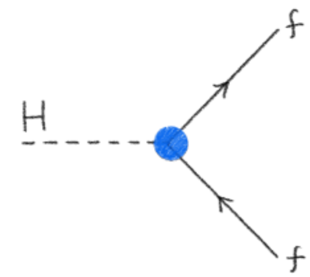

$$\boxed{A(\mathrm{Hff}) = -\frac{m_{\mathrm{f}}}{v}\bar{\psi}_{\mathrm{f}}\left(\kappa_{\mathrm{f}} + \mathrm{i}\,\tilde{\kappa}_{\mathrm{f}}\gamma_5\right)\psi_{\mathrm{f}}}$$

κ_{f} term is CP-even

$\tilde{\kappa}_{\mathrm{f}}$ term is CP-odd ~~CP~~

Both are tree-level (unlike HVV)

→ Define mixing angle ϕ, where $\boxed{\tan(\phi) = \frac{\tilde{\kappa}}{\kappa}}$

- pure CP-even state: ϕ=0º
- pure CP-odd state: ϕ=90º

EXPERIMENTAL RESULTS

Hττ

H→ττ: first direct measurement of the CP nature of the tau Yukawa coupling, by CMS (next slides)

Htt

- ttH (H→γγ): first experimental results last year ATLAS & CMS
- Combination of H→4l (ggH & ttH) with ttH (H→γγ), by CMS (next slides)

CMS-PAS-HIG-20-006

Using full Run 2 and exploiting $\tau_\mu\tau_h$ and $\tau_h\tau_h$ ch. (50% of the decay modes)

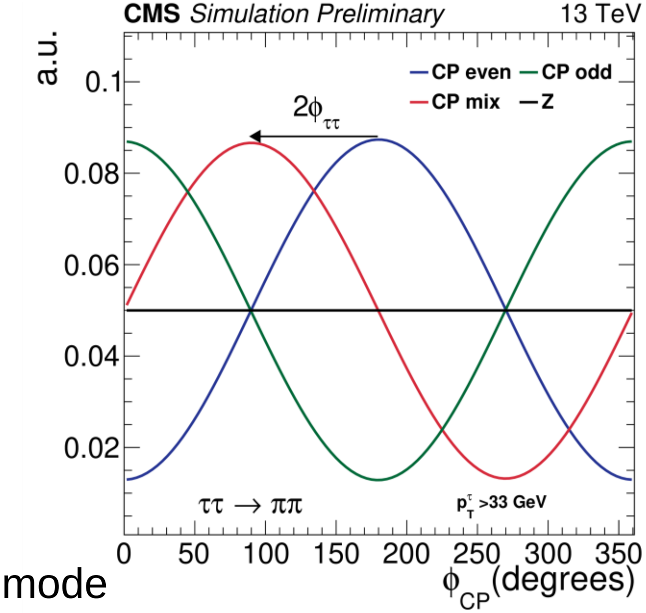

CP discriminant: ϕ_{CP}

(angle between the τ decay planes in the Higgs rest frame)

→ The mixing angle $\phi_{\tau\tau}$ can be extracted by fitting this function:

$$\frac{d\Gamma}{d\phi_{\mathrm{CP}}} \propto \cos(\phi_{\mathrm{CP}} - 2\phi_{\tau\tau})$$

assuming CP-even (SM) HVV couplings

Event reconstruction:

Dedicated algorithms and MVAs to reconstruct τ_h and distinguish its decay mode

Several channels $(\mu,\pi,\rho,a_1^{1pr},a_1^{3pr})\times(\pi,\rho,a_1^{1pr},a_1^{3pr})$

τ planes can't be reconstructed exactly → use approximations

$\tau_\mu \to \mu^\pm \nu\nu$ (17%)
$\tau_h \to \pi^\pm \nu$ (12%)

Impact parameter method: define planes using charged particle direction and its IP vector

$\to \rho^\pm \nu \to \pi^\pm \pi^0 \nu$ (26%)
$\to a_1^\pm \nu \to \pi^\pm \pi^0 \pi^0 \nu$ (10%) [1pr]
$\to a_1^\pm \nu \to \pi^\pm \rho^0 \nu \to \pi^\pm \pi^\pm \pi^\mp \nu$ (10%) [3pr]

Neutral pion method

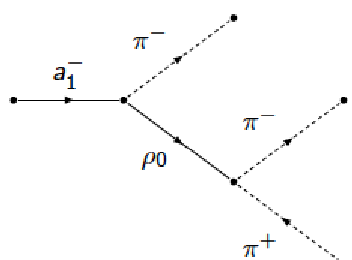

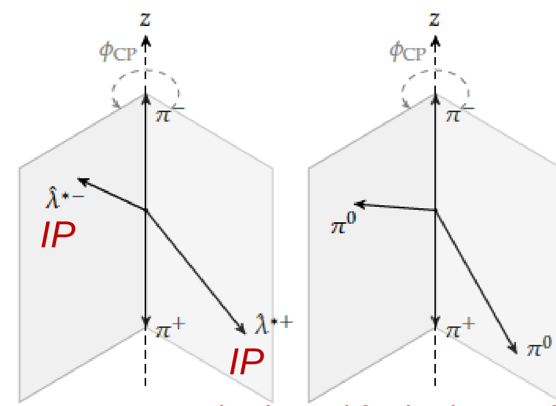

Impact parameter method used for both taus (left), π0 method used for both taus (right)

→ most sensitive: μρ, πρ, ρρ

$H\tau\tau$ coupling structure: analysis strategy

Main backgrounds: two genuine τ_h and jets faking τ_h, estimated with data-driven methods (embedding and fake factor, resp.)

Event categorisation:

- Signal vs background separation using multi-class BDT (DNN) for $\tau_h\tau_h$ ($\tau_\mu\tau_h$) ch.: includes invariant masses, kinematic and angular variables (e.g. $m_{\tau\tau}$ p_T's , m_{jj}, N_{jets}, etc.)
- 3 categories: Higgs (VBF + ggH + VH), genuine τ_h ($Z\rightarrow\tau\tau$ embedded) and fake τ_h
- For events classified as Higgs, ϕ_{CP} unrolled distribution in BDT/DNN score windows (for each decay mode) used to extract CP information

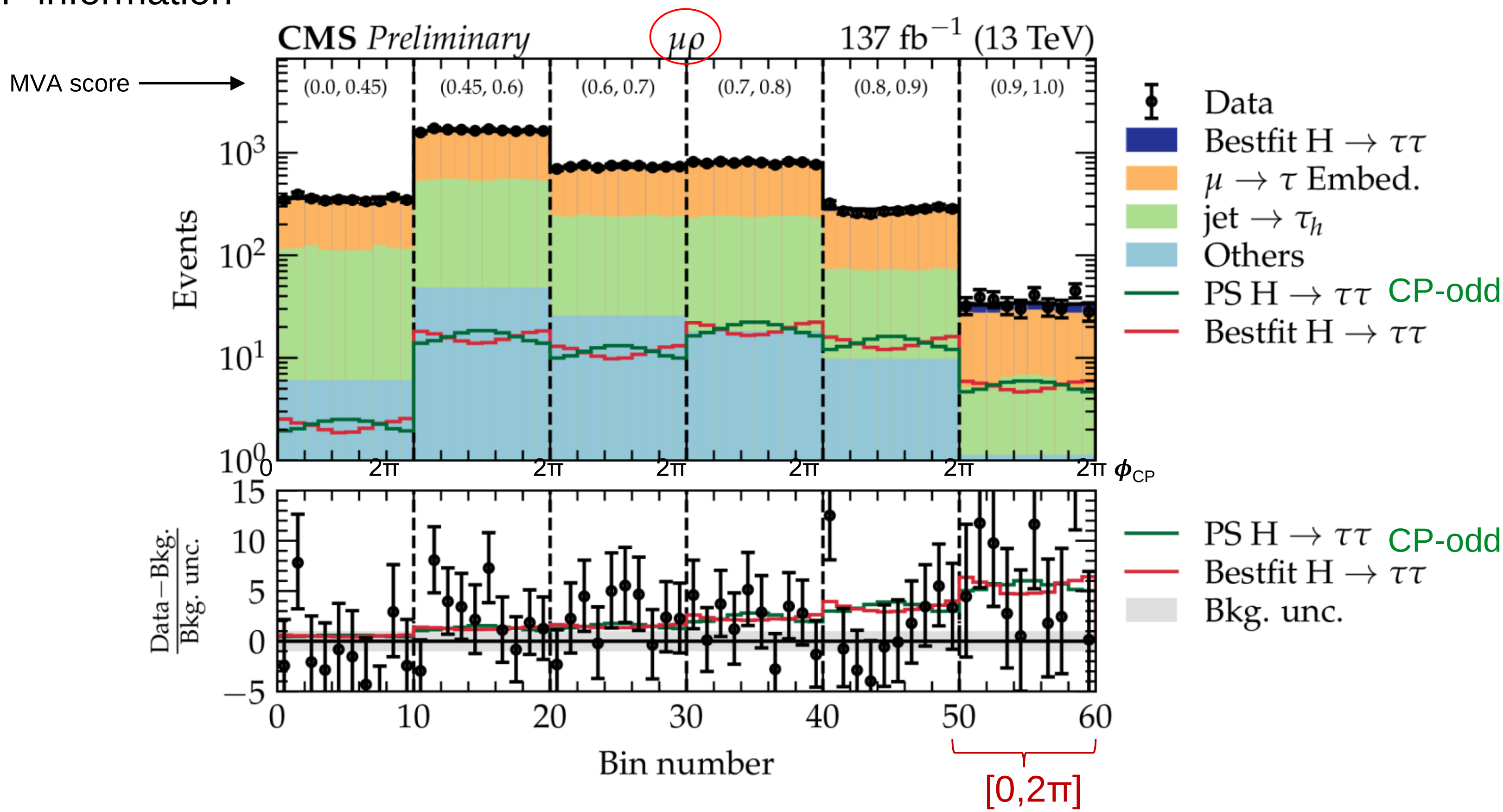

Results: simultaneous maximum likelihood fit of $\boldsymbol{\phi}_{CP}$ unrolled dist. (and CRs) to extract CP state information

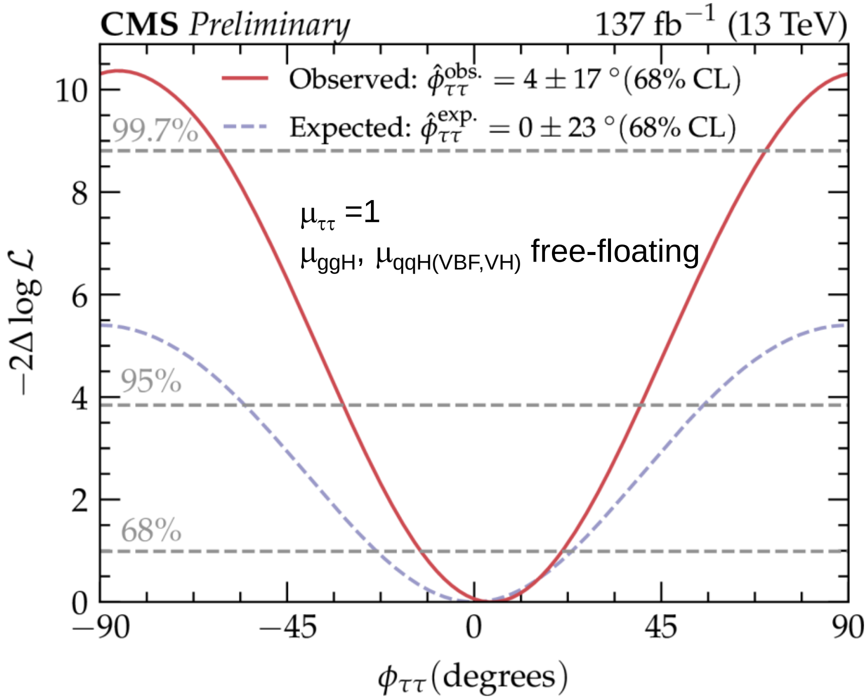

$$L(\vec{\mu}, \mu^{\tau\tau}, \phi_{\tau\tau}, \vec{\theta})$$

$$\vec{\mu} = (\mu_{ggH}, \mu_{qqH})$$

$\mu^{\tau\tau}$: H→ττ BR modifier

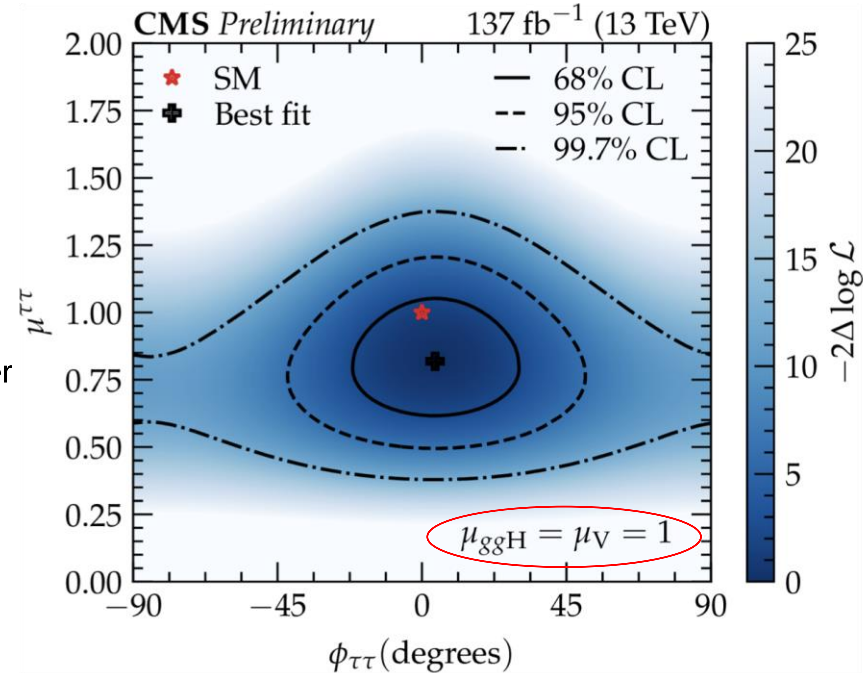

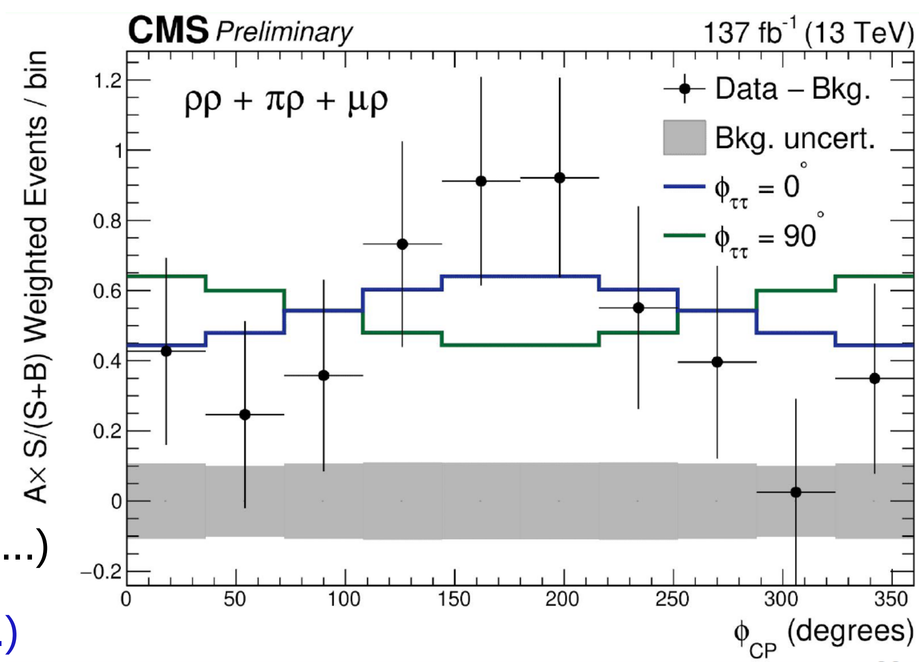

- $\boldsymbol{\phi}_{\tau\tau}$ **compatible with zero:** $\phi_{\tau\tau}$= (4±17)º @68%CL
  |ϕ|<36º @95%CL
  (nMSSM |ϕ|<27º → this result excludes a part of the phase-space of this model @68%CL)

- Measurement limited by data statistics
  (main syst unc.: hadronic tau trigger, theory, tau enery scale...)

- A pure CP-odd Hττ coupling excluded with 3.2σ (2.3σ exp.)

Probing Hgg coupling structure in H→WW*→eνμν + 2 jets

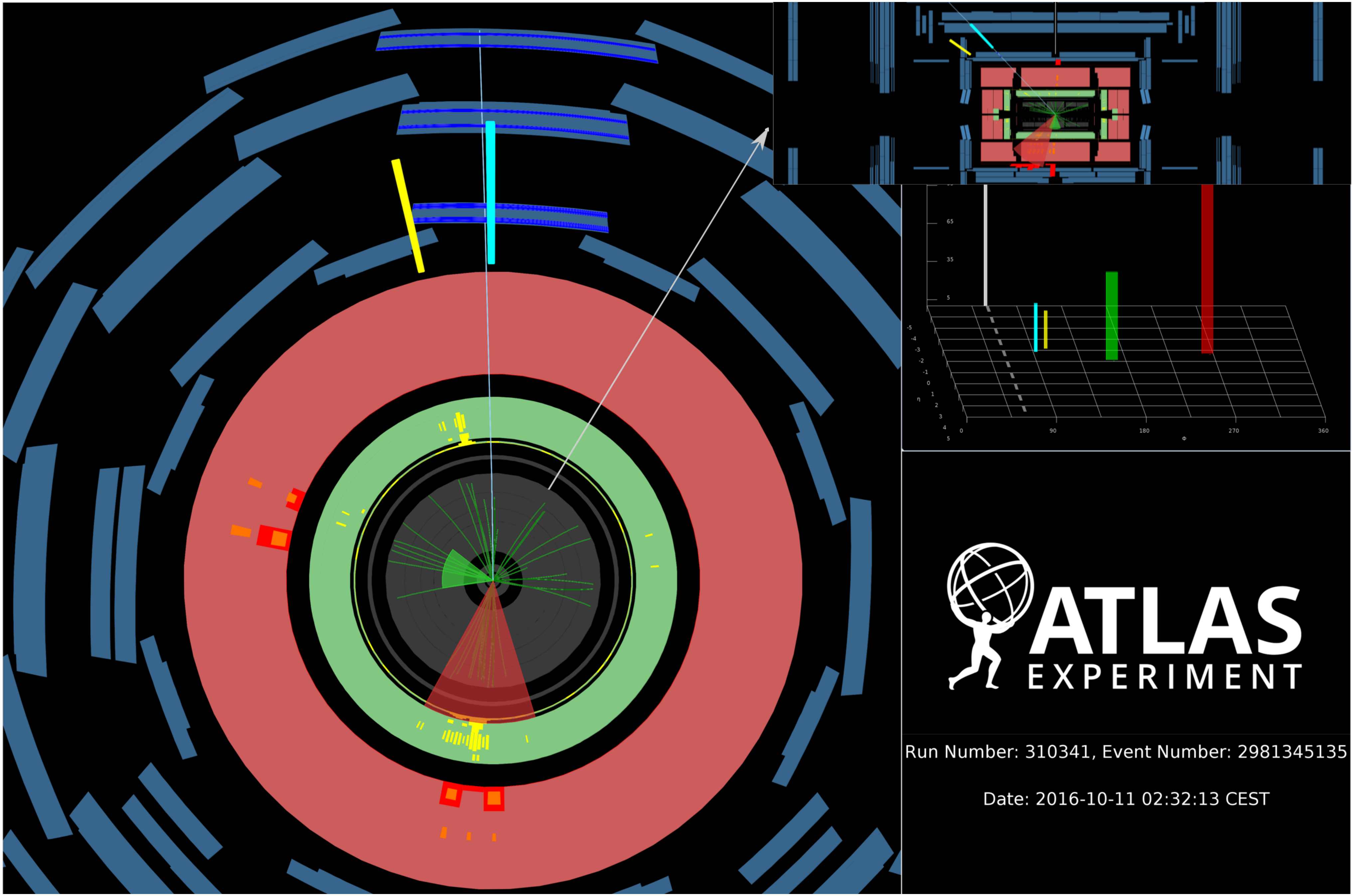

Probing Hgg coupling structure in H→WW*→eνμν + 2 jets

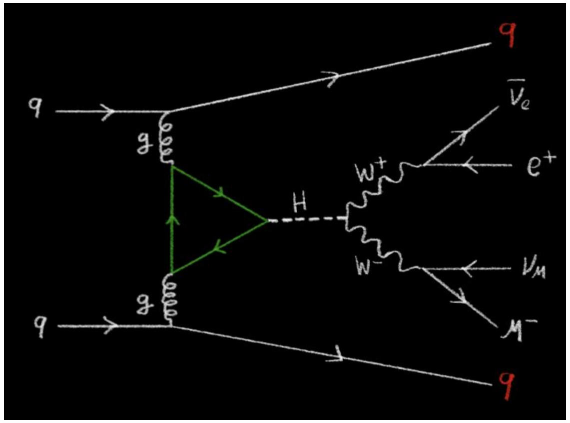

ATLAS-CONF-2020-055

Higgs boson produced through gluon fusion (+2 jets)
Constrain the properties of the **effective Higgs-gluon interaction**
Higgs Characterization model provides EFT framework

CP-even coupling strength scale factor — CP-odd coupling strength scale factor

$$\mathcal{L}_0^{\text{loop}} = -\frac{1}{4}\left(\kappa_{Hgg} g_{Hgg} G^a_{\mu\nu} G^{a,\mu\nu} + \kappa_{Agg} g_{Hgg} G^a_{\mu\nu} \tilde{G}^{a,\mu\nu}\right) H$$

CP discriminant: $\Delta\phi_{jj}$
(signed azimuthal angle difference of the two jets)

$$\Delta\Phi_{jj} = \begin{cases} \phi_{j_1} - \phi_{j_2} \text{ if } \eta_{j_1} > \eta_{j_2} \\ \phi_{j_2} - \phi_{j_1} \text{ otherwise} \end{cases}$$

$< \Delta\phi_{jj} - \pi > != 0$ would indicate CP-mixed state

assuming CP-even (SM) HVV couplings

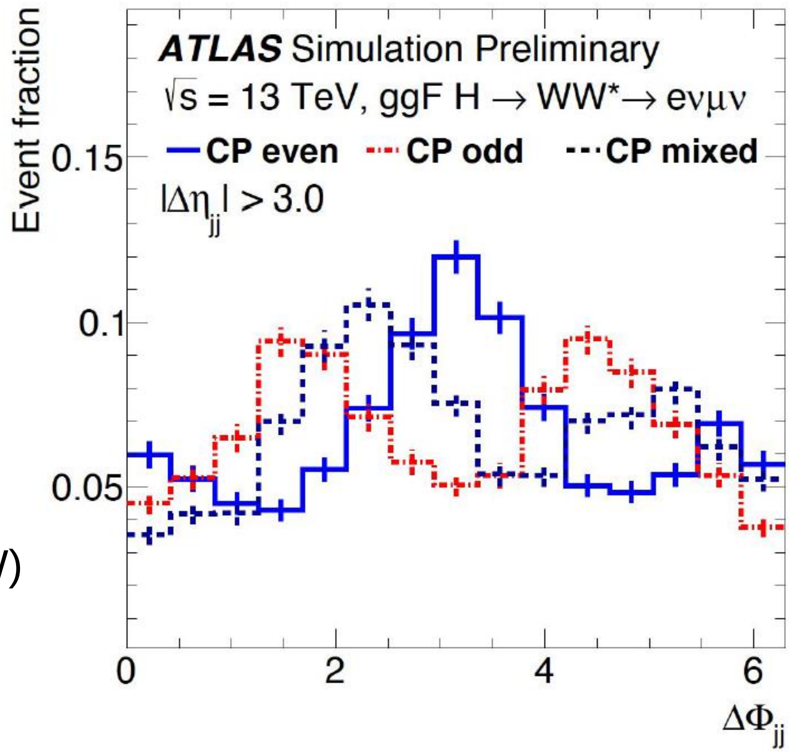

Event selection and categorisation:
Preselection: 2 OS DF leptons, ≥ 2 jets
+ cuts on kinematics of di-lepton system, ΔR_{jj}, veto b-jets

BDTs to further separate signal from main bkgs. (top, $Z\rightarrow\tau\tau$ & WW)
- trained using kinematics of di-lepton system and angular distances between leptons and jets
- low BDT region used to constrain normalisation of main bkgs.

Probing Hgg coupling structure in H→WW*→$e\nu\mu\nu$ + 2 jets

ATLAS-CONF-2020-055

Results: fit to $\Delta\phi_{jj}$ observable in 12 event cat (3 BDT x 4 $|\Delta\eta_{jj}|$)
Bkgs. norm. constrained with dedicated CR & low BDT bins

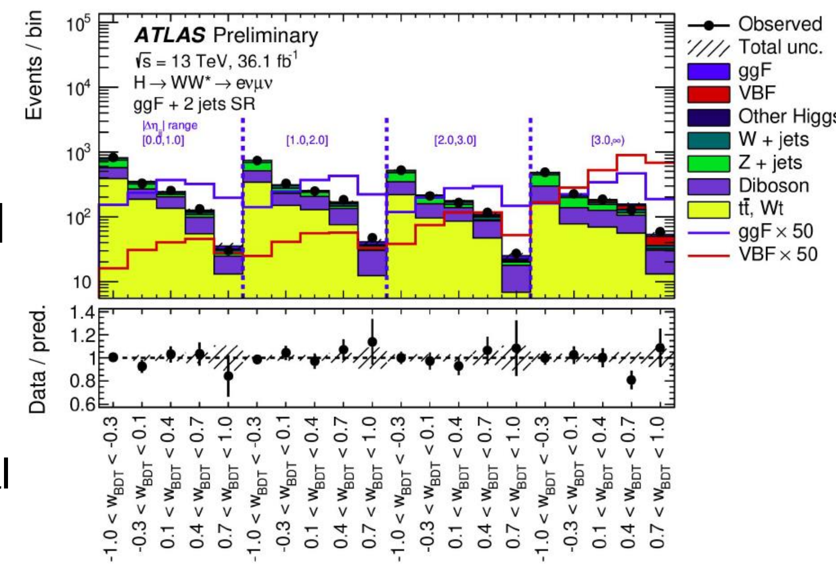

shape+rate fit (constraining signal norm. to model predictions)
[if signal norm. is free, data not sensitive enough to give 68%CL]

$$\kappa_{Agg}/\kappa_{Hgg} = 0.0 \pm 0.4(\text{stat.}) \pm 0.3(\text{syst.})$$

Stat. limited (only a fraction of LHC Run 2 dataset used)
Dominant syst. unc: modelling of top & WW bkgs, and ggF signal

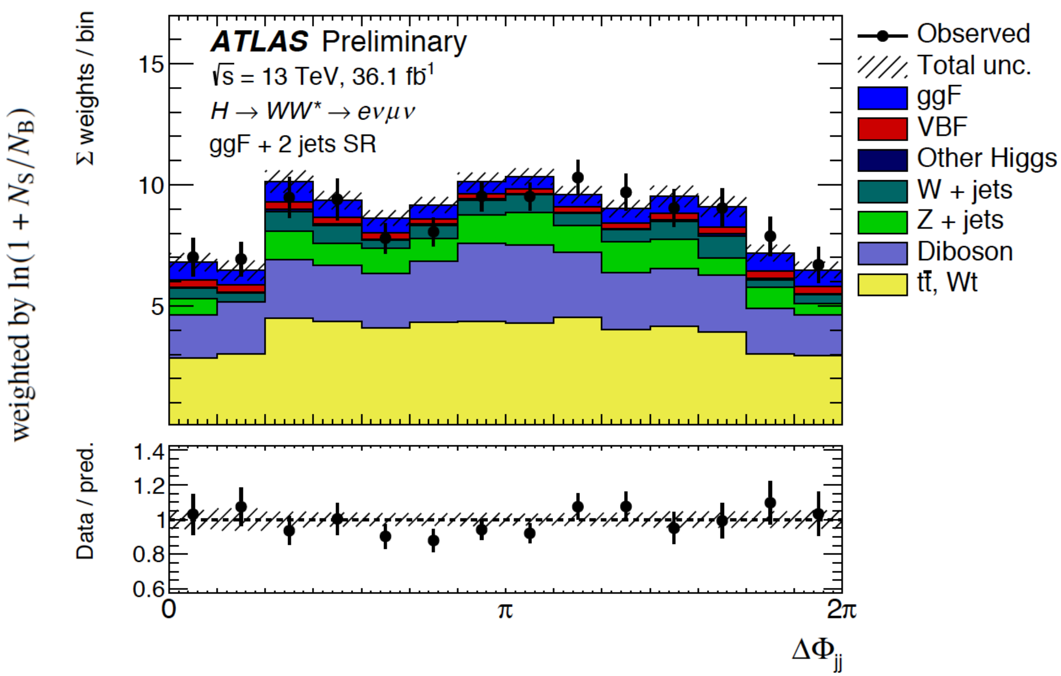

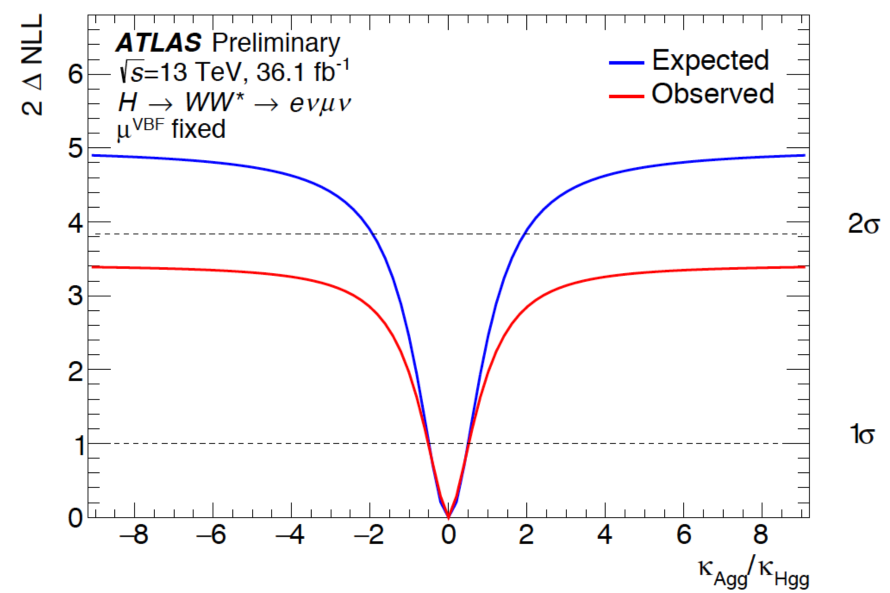

First measurement of polarisation effects in HVV also presented in this note (using VBF production)!

H→4l to probe HVV, Hgg and Htt couplings

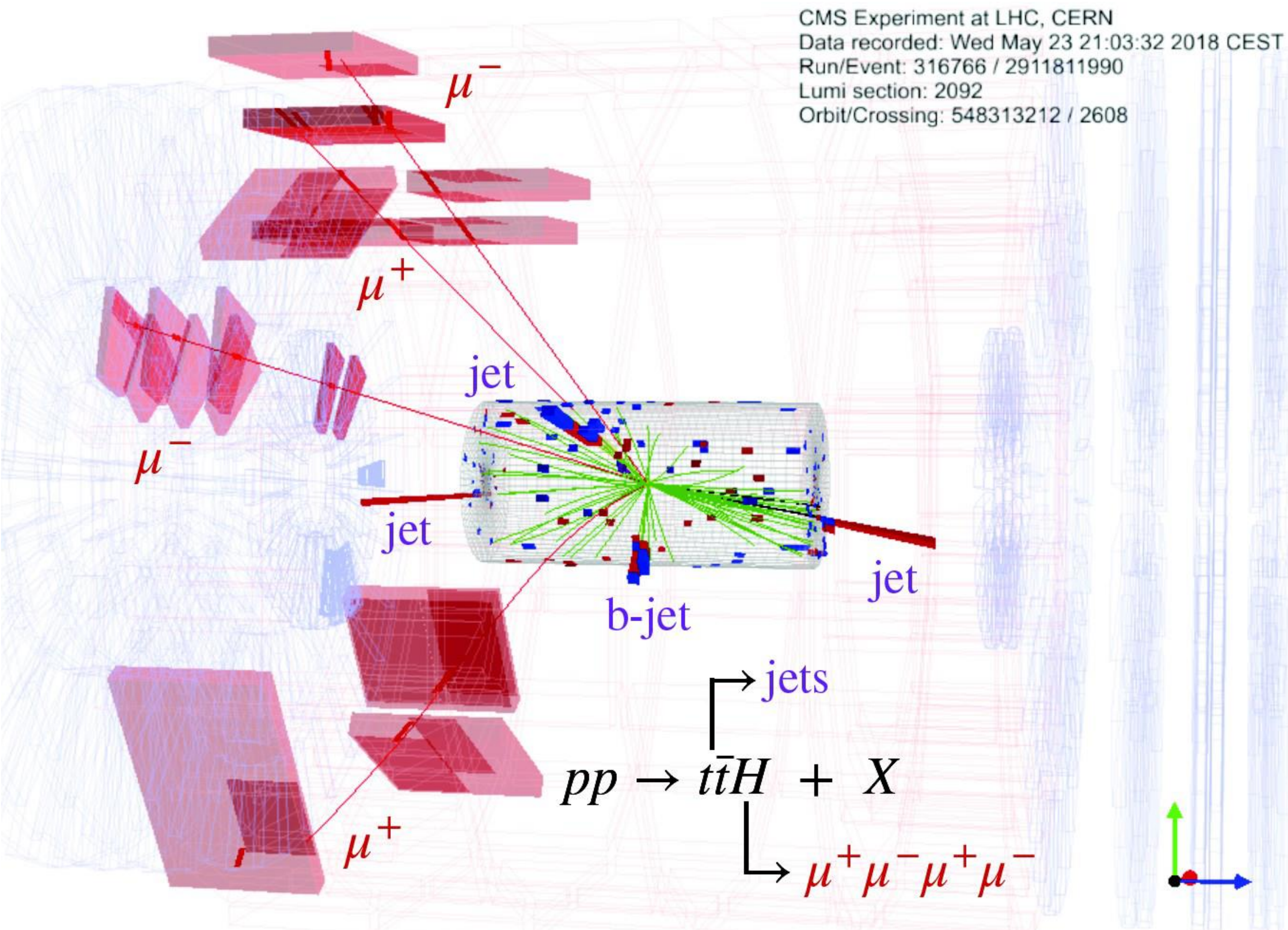

H→4l to probe HVV, Hgg and Htt couplings

arXiv:2104.12152

All production modes of H→4l (2e2μ, 4μ, 4e) assessed → test HVV, Hgg & Htt interactions
Dedicated measurement → MC simulation of new physics, including acceptance and efficiency effects
Amplitudes parametrised with anomalous couplings → translated to EFT coef. (Higgs and Warsaw bases)

Generic HV_1V_2 scattering amplitude *V_1V_2=ZZ,WW, Zγ, $\gamma\gamma$ or gg*

tree-level SM-like | CP-even anomalous couplings | CP-odd anomalous coupling

$$A(\mathrm{HV_1V_2}) \sim \left[a_1^{\mathrm{VV}} + \frac{\kappa_1^{\mathrm{VV}} q_1^2 + \kappa_2^{\mathrm{VV}} q_2^2}{\left(\Lambda_1^{\mathrm{VV}}\right)^2} \right] m_{\mathrm{V1}}^2 \epsilon_{\mathrm{V1}}^* \epsilon_{\mathrm{V2}}^* + a_2^{\mathrm{VV}} f_{\mu\nu}^{*(1)} f^{*(2)\mu\nu} + a_3^{\mathrm{VV}} f_{\mu\nu}^{*(1)} \tilde{f}^{*(2)\mu\nu}$$

SM: a_1^{ZZ}, a_1^{WW}, a_2^{gg}
Others: anomalous couplings

Generic Hff scattering amplitude

$$A(\mathrm{Hff}) = -\frac{m_{\mathrm{f}}}{v} \bar{\psi}_{\mathrm{f}} \left(\kappa_{\mathrm{f}} + \mathrm{i}\,\tilde{\kappa}_{\mathrm{f}} \gamma_5\right) \psi_{\mathrm{f}}$$

→ coupling ratios can be defined:

$$f_{ai}^{\mathrm{VV}} = \frac{|a_i^{\mathrm{VV}}|^2 \alpha_{ii}^{(2e2\mu)}}{\sum_j |a_j^{\mathrm{VV}}|^2 \alpha_{jj}^{(2e2\mu)}} \,\mathrm{sign}\left(\frac{a_i^{\mathrm{VV}}}{a_1}\right)$$

$$f_{a3}^{\mathrm{ggH}} = \frac{|a_3^{\mathrm{gg}}|^2}{|a_2^{\mathrm{gg}}|^2 + |a_3^{\mathrm{gg}}|^2} \,\mathrm{sign}\left(\frac{a_3^{\mathrm{gg}}}{a_2^{\mathrm{gg}}}\right)$$

$$f_{\mathrm{CP}}^{\mathrm{Hff}} = \frac{|\tilde{\kappa}_{\mathrm{f}}|^2}{|\kappa_{\mathrm{f}}|^2 + |\tilde{\kappa}_{\mathrm{f}}|^2} \,\mathrm{sign}\left(\frac{\tilde{\kappa}_{\mathrm{f}}}{\kappa_{\mathrm{f}}}\right)$$

Event categorisation

Using kinematic discriminants, calculated with matrix element likelihood approach (MELA), sensitive to distinguish each production mode (S-vs-B), and also other selection requirements (p_T^{4l})

→ two indep. sets of event categories:
- scheme 1: targets Hgg and Htt (7 categories)
- scheme 2: targets HVV (6 categories)

→ two type of discriminants:

$$\mathcal{D}_{\mathrm{alt}}(\Omega) = \frac{\mathcal{P}_{\mathrm{sig}}(\Omega)}{\mathcal{P}_{\mathrm{sig}}(\Omega) + \mathcal{P}_{\mathrm{alt}}(\Omega)}$$

to separate S-vs-B or SM-vs-BSM couplings

$$\mathcal{D}_{\mathrm{int}}(\Omega) = \frac{\mathcal{P}_{\mathrm{int}}(\Omega)}{2\sqrt{\mathcal{P}_{\mathrm{sig}}(\Omega)\,\mathcal{P}_{\mathrm{alt}}(\Omega)}}$$

to assess interference btw. two model predictions (eg. CP-even/odd)

H→4l to probe HVV, Hgg and Htt couplings

arXiv:2104.12152

CP discriminants: kinematic dist. obtained with MELA

For each event cat., few observables D_{alt} (and D_{int}) are defined:

- the full kinematic information from each event (production, decay and interference information) is exploited
- a complete set of mass and angular input observables Ω used:

$$\Omega^{\rm dec} = \{\theta_1, \theta_2, \Phi, \theta^*, \Phi_1, m_1, m_2, m_{4\ell}\}$$

$\Omega^{\rm prod}$ for the ggH, VBF, VH, and $t\bar{t}H$ production

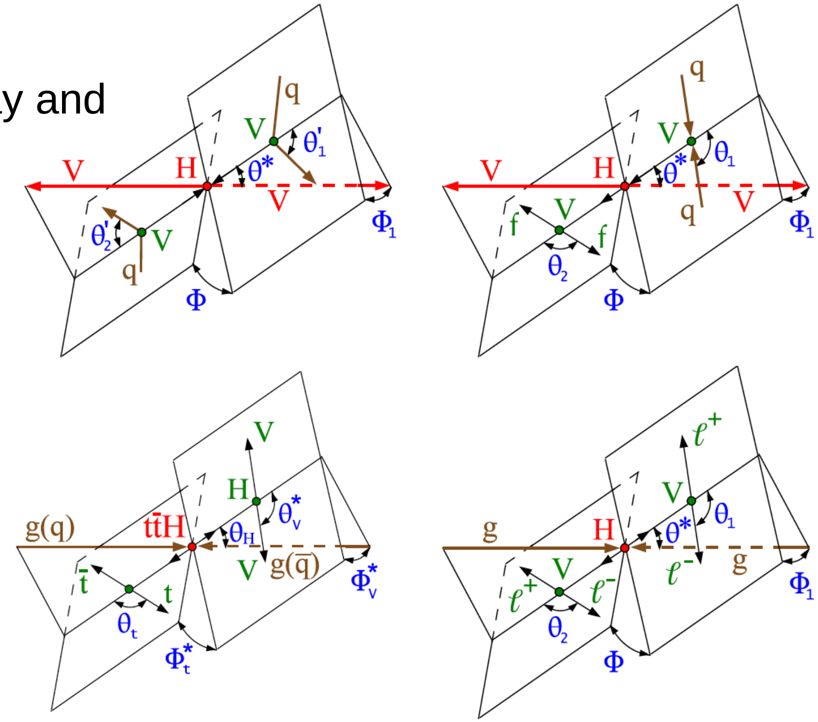

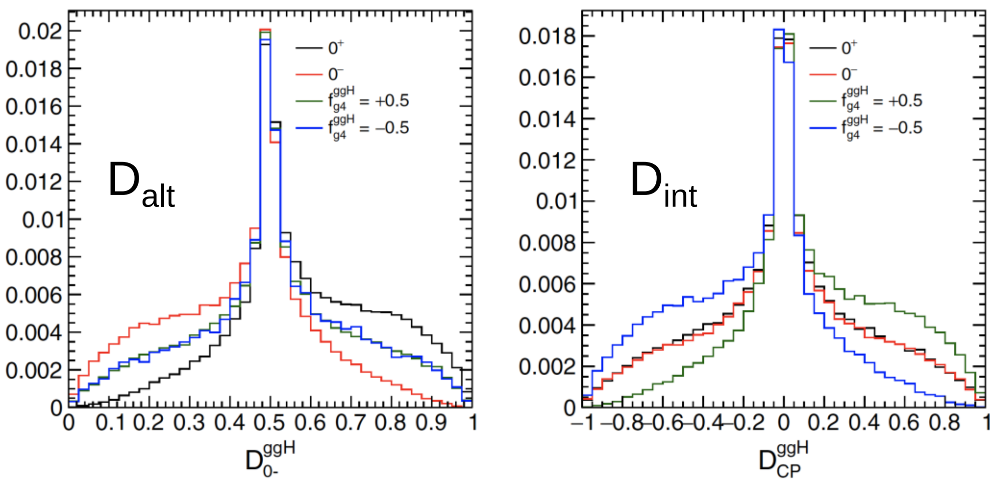

PRD102, 056022 (2020)

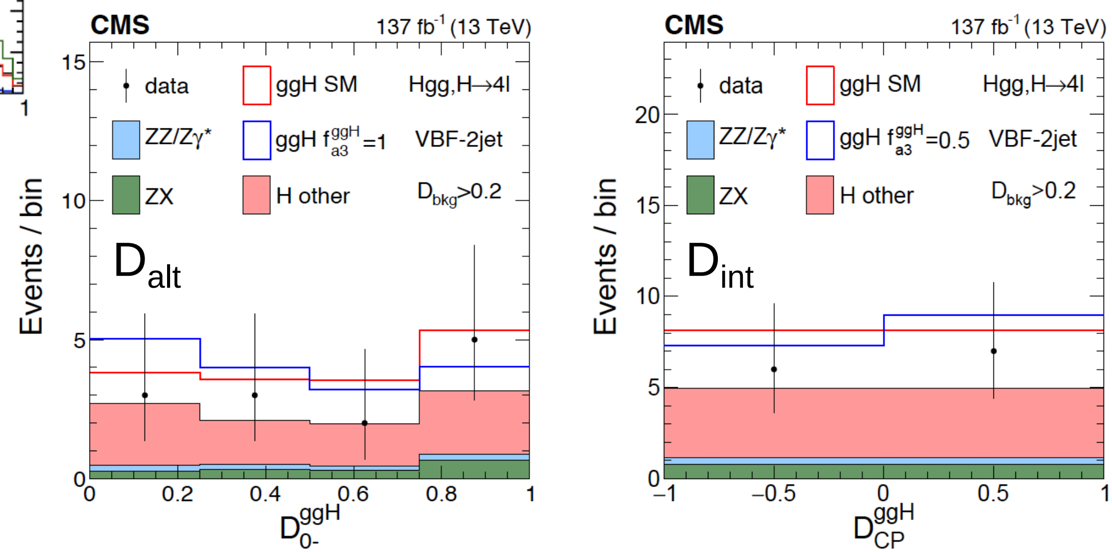

H→4l to probe HVV, Hgg and Htt couplings

arXiv:2104.12152

Results:

- Perform maximum likelihood fits to to extract the coupling ratios f_i (and μ_i)

$$\mathcal{P}_k(\vec{x}) = \sum_j \mu_j \mathcal{P}^{\mathrm{sig}}_{jk}\left(\vec{x}; \vec{\xi}_{jk}, \vec{f}_j\right) + \sum_i \mathcal{P}^{\mathrm{bkg}}_{ik}\left(\vec{x}; \vec{\xi}_{ik}\right)$$

- 3 types of scans:
  - Single parameter scans with other couplings fixed
  - Simultaneous scans of multiple anomalous couplings
  - 2D scans

- Translate couplings ratios f_i into EFT coefficients

HVV couplings (within SU(2)xU(1) symmetry)

Coupling amplitude decomposition

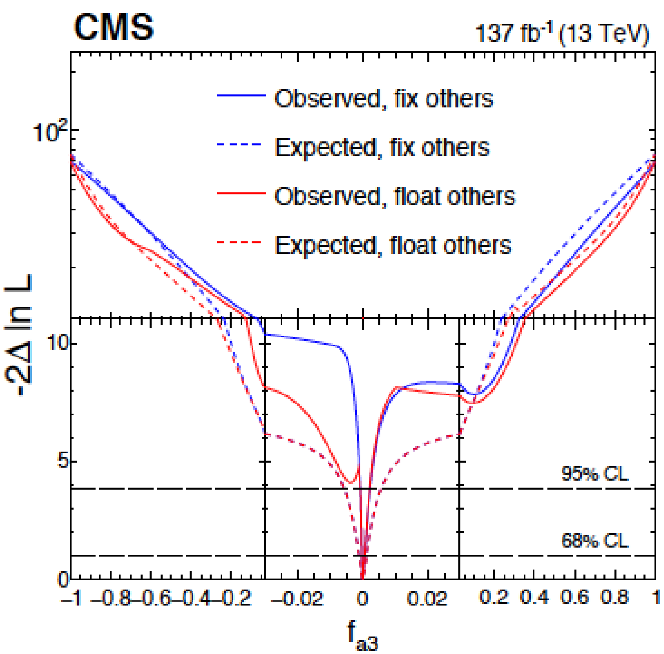

Higgs basis of SMEFT

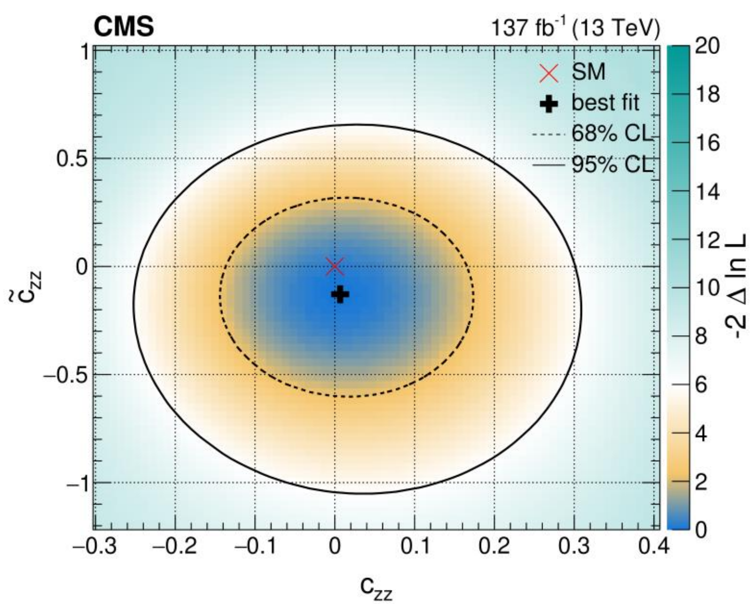

Channels VBF & VH & $H \to 4\ell$

Coupling	Observed
δc_z	$-0.03^{+0.06}_{-0.25}$
c_{zz}	$0.01^{+0.11}_{-0.10}$
$c_{z\Box}$	$-0.02^{+0.04}_{-0.04}$
$\tilde{c}_{zz}$	$-0.11^{+0.30}_{-0.31}$

c_{gg} and $\tilde{c}_{gg}$ couplings left unconstrained.

Results consistent with SM Higgs

arXiv:2104.12152

Hgg and Htt couplings

$$\frac{\sigma(\mathrm{ggH})}{\sigma_{\mathrm{SM}}} = \kappa_{\mathrm{f}}^2 + 2.38\tilde{\kappa}_{\mathrm{f}}^2$$

Higgs basis of SMEFT

Channels	Coupling	Observed
	c_{gg}	$-0.0012^{+0.0022}_{-0.0174}$
tH & $\mathrm{t\bar{t}H}$ & ggH	$\boxed{\tilde{c}_{gg}}$	$\boxed{-0.0017^{+0.0160}_{-0.0130}}$
	κ_t	$1.05^{+0.25}_{-0.20}$
	$\boxed{\tilde{\kappa}_t}$	$\boxed{-0.01^{+0.69}_{-0.67}}$

($\gamma\gamma$ + 4l)

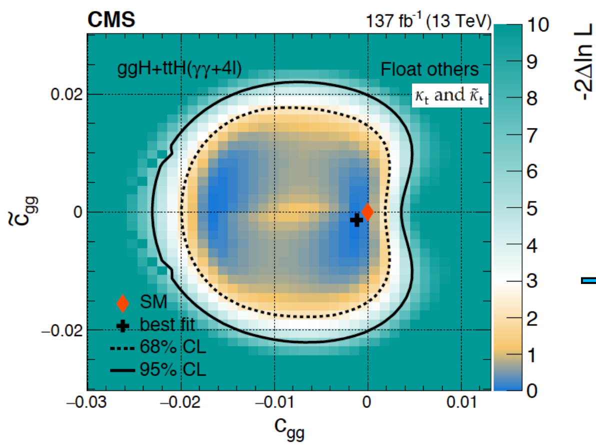

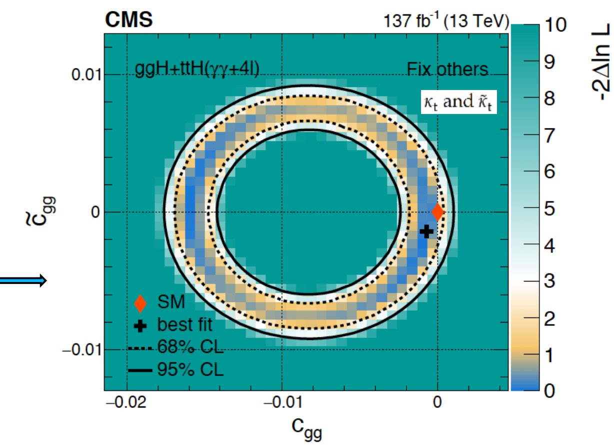

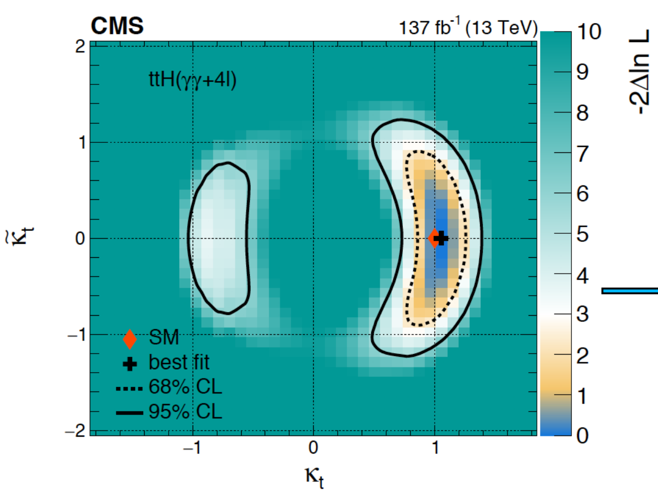

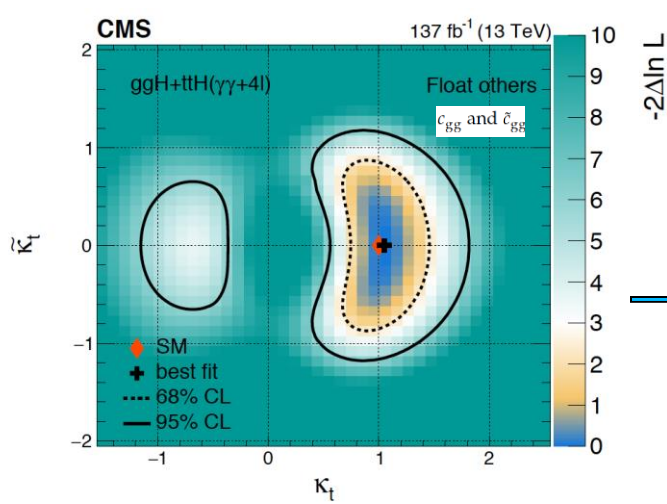

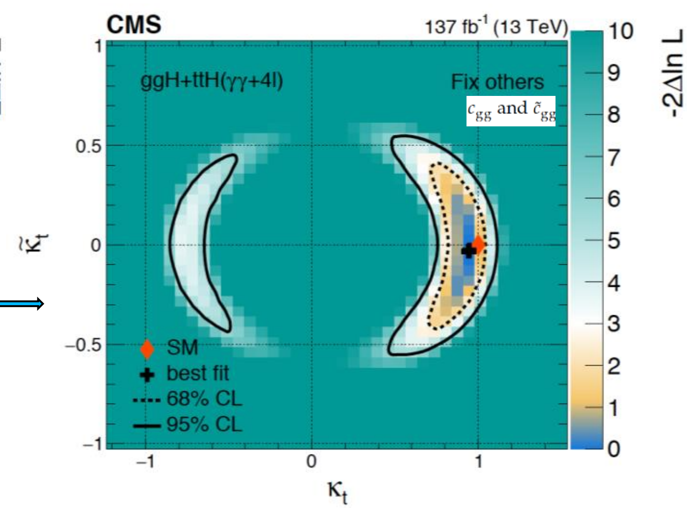

Results consistent with SM Higgs

Understanding the Higgs boson’s CP properties is a crucial aspect in particle physics today.

ATLAS and CMS have looked for BSM contributions and set limits on CP anomalous couplings in the Higgs boson interactions with vector bosons (HVV), gluons (Hgg), and fermions (Hff).
Results are limited by statistical unc. and, so far, they are consistent with SM.
Purely CP-odd fermionic and bosonic Higgs couplings already excluded, but admixtures still possible.

Need to keep exploring CP violation in Higgs couplings.
A huge improvement is expected with more data from upcoming future LHC runs ☺
For the moment, neglecting effect of operators on backgrounds...

Zoom meeting

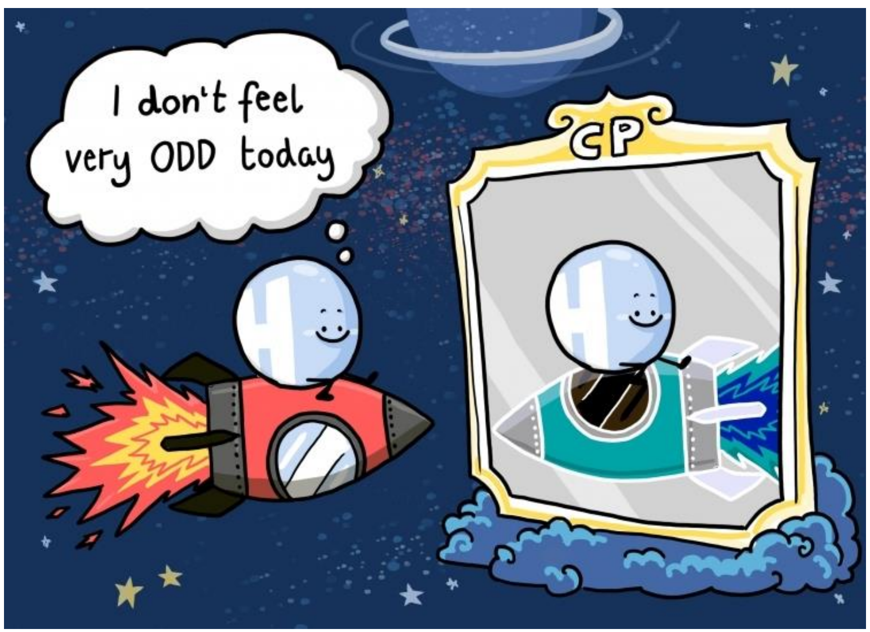

(image: DESY/designdoppel)

Discussions between theorists and experimentalists are very much appreciated !

THANKS FOR YOUR ATTENTION

maria.moreno.llacer@cern.ch

- Higgs decay probability ($\beta_\tau = 1$):

$$\Gamma_{h\to\tau^-\tau^+} \sim 1 - \vec{s}_z^{\,-}\vec{s}_z^{\,+} + \underbrace{\cos(2\phi_h)(\vec{s}_T^{\,-}\vec{s}_T^{\,+})}_{\text{CP even}} - \underbrace{\sin(2\phi_h)[(\vec{s}_T^{\,-}\times\vec{s}_T^{\,+})\cdot\hat{k}^{\tau^-}]}_{\text{CP odd}}$$

- $\vec{s}_{z,T}^{\,\pm}$ - longitudinal, transverse vectors of $\tau^\pm$ spin in its rest frame with respect to $\hat{k}^{\tau^-} = \hat{e}_z$
- Higgs CP information encoded in the transverse component
- $$\frac{1}{\Gamma}\frac{d\Gamma(h\to\pi^+\pi^- + 2\nu)}{d\varphi^*_{CP}} = \frac{1}{2\pi}\left[1 - \frac{\pi^2}{16}\cos(\varphi^*_{CP} - 2\phi_h)\right]$$

- $2\phi_h$ can be determined from the shift of the fitted φ_{CP} distribution with respect to the red curve for which $\phi_h = 0$.
- Precision on ϕ_h depends on the number of events and the size of the amplitude

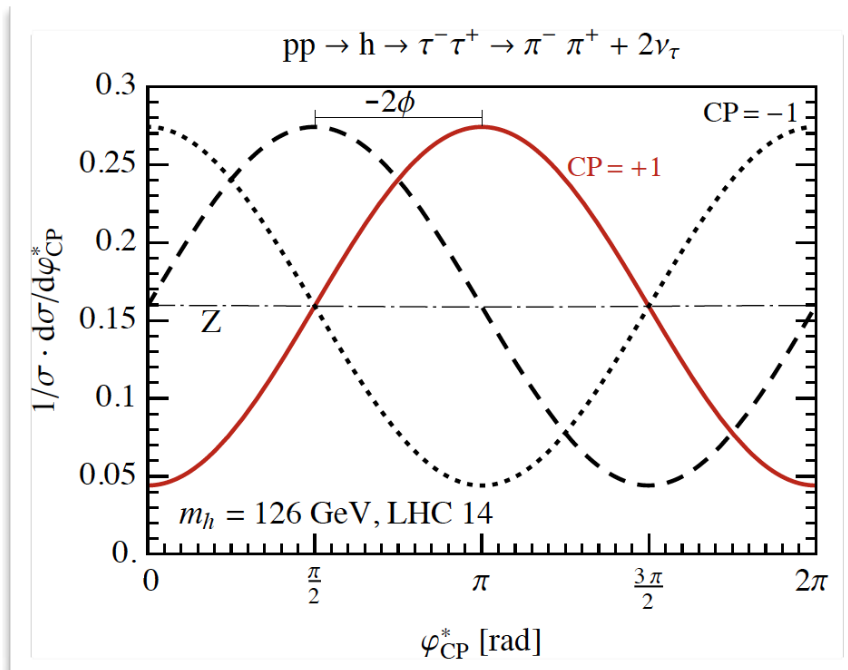

Backgrounds

Table 3: The different sources of di-τ backgrounds are depicted on the rows and columns. The entries in the table represent the possible di-τ background contribution from different processes and misidentifications and encapsulate the different experimental techniques that are deployed to estimate the background contributions. Processes involving two prompt leptons, i.e. two electrons, muons, or and electron and a muon, are not considered in this analysis.

	genuine τ_h	jet$\rightarrow\tau_h$	lepton$\rightarrow\tau_h$
genuine τ	τ-Embedding		
jet$\rightarrow\tau$	Fake Factor	Fake Factor	
lepton$\rightarrow\tau$	Simulation	Fake Factor	Simulation
prompt lepton	Simulation	Fake Factor	Simulation

Table 4: Input variables to the MVA discriminants for the $\tau_\mu\tau_h$ and $\tau_h\tau_h$ channel. For all variables only the visible decay products of the τ leptons are implied, except for the $\tau_\mu\tau_h$ and $\tau_h\tau_h$ mass, for which the SVFIT algorithm is used.

Input variables to MVAs

The training is performed inclusively for all the τ decay modes.

Observable	$\tau_\mu\tau_h$	$\tau_h\tau_h$
p_T of leading τ_h or τ_μ	✓	✓
p_T of (trailing) τ_h for $\tau_\mu\tau_h$ ($\tau_h\tau_h$) channel	✓	×
p_T of visible di-τ	✓	✓
p_T of di-τ_h + p_T^{miss}	×	✓
p_T of $\mu + \tau_h + p_T^{miss}$	✓	×
Visible di-τ mass	✓	✓
$\tau_\mu\tau_h$ or $\tau_h\tau_h$ mass (using SVFIT)	✓	✓
Leading jet p_T	✓	✓
Trailing jet p_T	✓	×
Jet multiplicity	✓	✓
Dijet invariant mass	✓	✓
Dijet p_T	✓	×
Dijet $\lvert\Delta\eta\rvert$	✓	×
p_T^{miss}	✓	✓

$H\tau\tau$

CMS-PAS-HIG-20-006

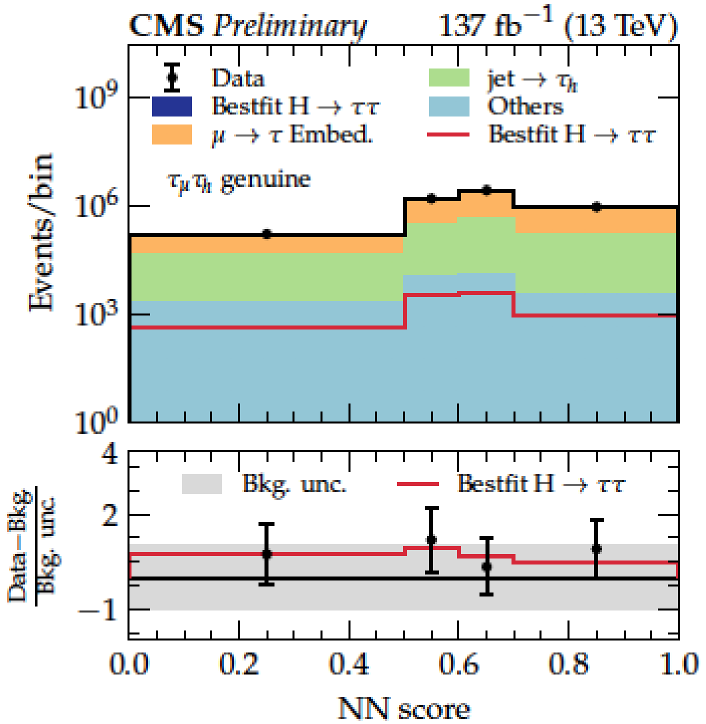

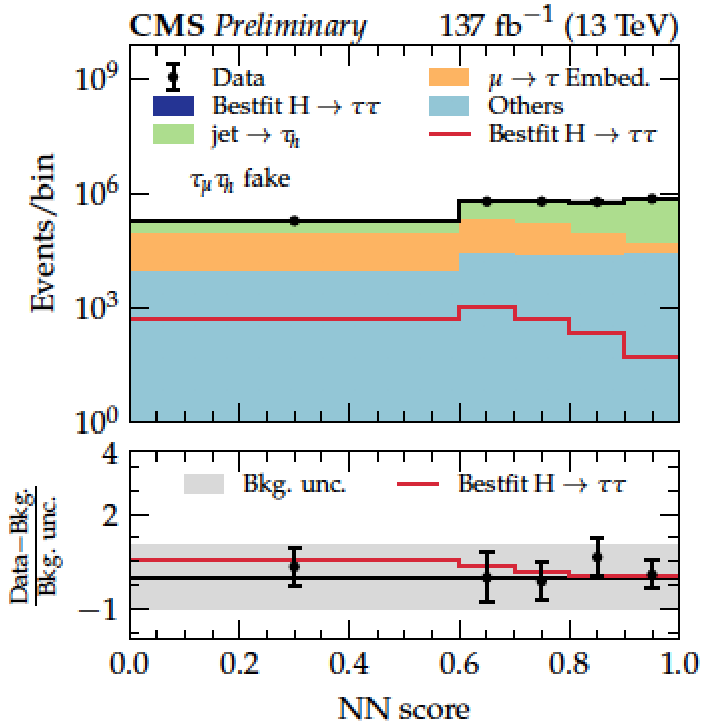

Distributions are inclusive in τ decay mode.

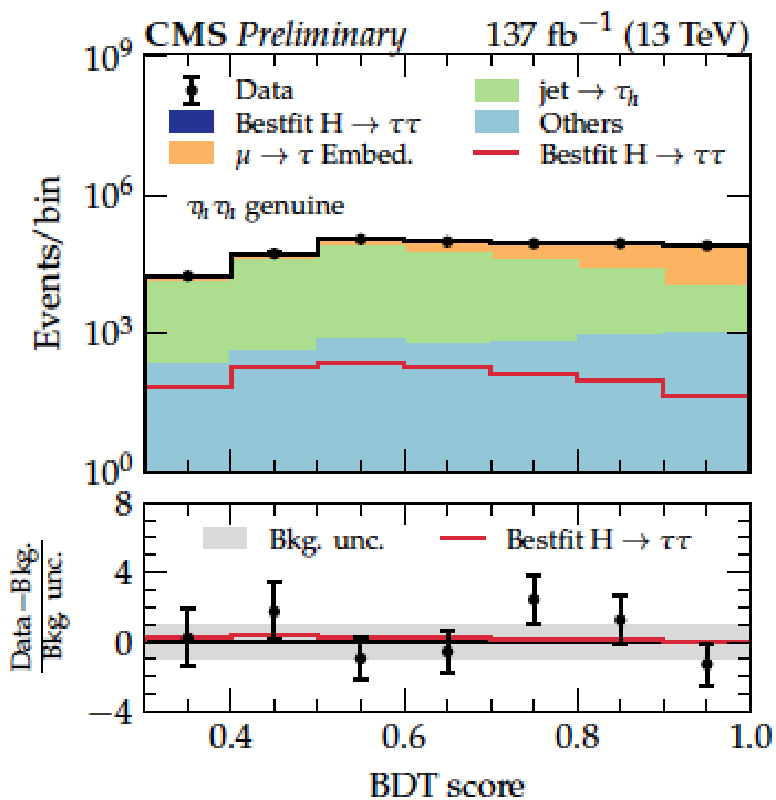

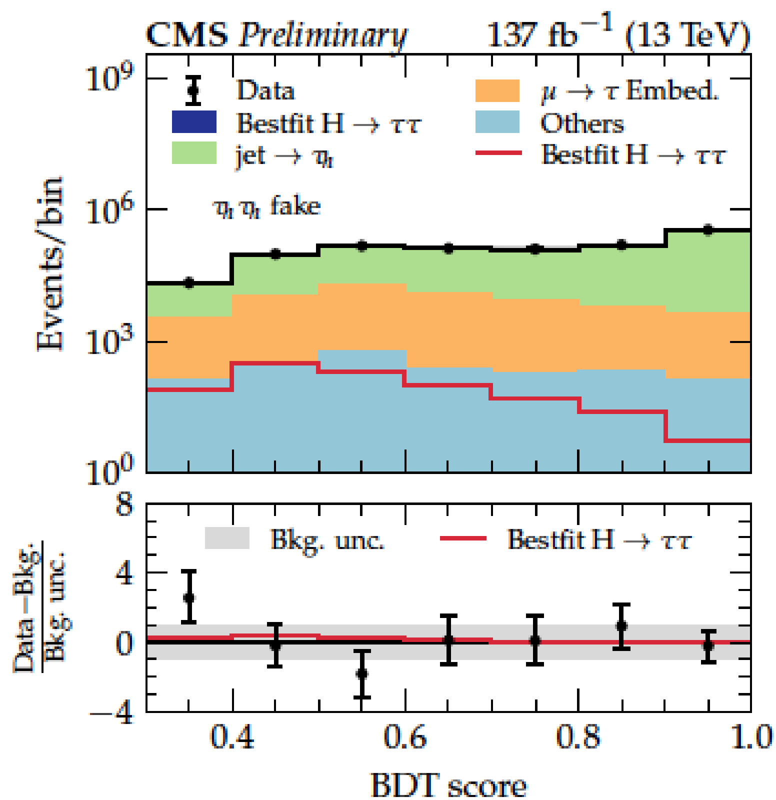

CMS-PAS-HIG-20-006

Decay mode	Expected sensitivity
$\tau_\mu \tau_h$	1.47
$\mu\rho$	1.16
$\mu\pi$	0.71
μa_1^{3pr}	0.51
μa_1^{1pr}	0.24
$\tau_h \tau_h$	1.8
$\rho\rho$	1.09
$\rho\pi$	1.04
ρa_1^{3pr}	0.64
$\pi\pi$	0.38
πa_1^{3pr}	0.46
$a_1^{1pr}\rho$ and $a_1^{1pr} a_1^{1pr}$	0.30
πa_1^{1pr}	0.23
$a_1^{3pr} a_1^{3pr}$	0.13
$a_1^{3pr} a_1^{1pr}$	0.11
Combined	2.33

Higgs CP

- With all final state particles reconstructed, we can perform a Matrix Element based analysis of the underlying Higgs CP mixing angle Φ. The Higgs decay amplitude can be expressed as

$$|\mathcal{M}|^2 \propto A + B\cos(2\phi) + C\sin(2\phi),$$
$$\propto I_1\cos^2(\phi) + I_2\sin(\phi)\cos(\phi) + I_3\sin^2(\phi)$$

- Two observables can be reconstructed per event for the CP test
  - Optimal Observable (M. Davier et. al, Phys. Lett. B306,1993, 411): OO = I_2/I_1
  - ME angle $\Delta\Phi_{ME}$, defined as

$$|\mathcal{M}|^2 \propto A + \sqrt{B^2+C^2}\cos(\Delta\phi_{ME} - 2\phi)$$
$$\cos(\Delta\phi_{ME}) = \frac{B}{\sqrt{B^2+C^2}}, \quad \sin(\Delta\phi_{ME}) = \frac{C}{\sqrt{B^2+C^2}}$$

At low mixing angle values, the two perform similarly, while in high values of Φ, $\Delta\Phi_{ME}$ is better

Xin Chen @ Americas Workshop on Linear Colliders 2017

CP test in H→ττ decay

- CP-odd Yukawa coupling can enter the Lagrangian at dim-4, thus sensitive at tree-level rather than with the dim-6 operators in HVV

$$-g_\tau\left(\cos\phi\bar{\tau}\tau+\sin\phi\bar{\tau}i\gamma_5\tau\right)h$$

Φ is the mixing angle. Φ=0 (Φ=π/2) means SM (CP odd)

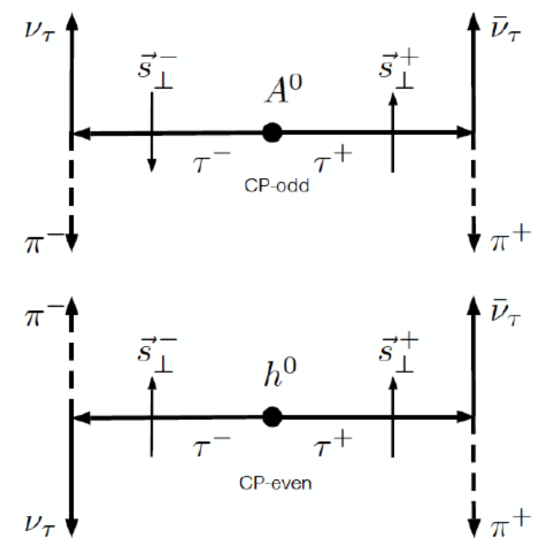

- CP of Hττ coupling can be distinguished by the transverse tau spin correlations

$$\Gamma(H,A\to\tau^-\tau^+)\ \sim\ 1-s_z^{\tau^-}s_z^{\tau^+}\boxed{\pm\, s_T^{\tau^-}\, s_T^{\tau^+}}$$

Sensitive to CP (H vs A)

- For example, with the τ→πν decay, one can look at the angle between tau decay planes to extract Φ:

$$\frac{d\Gamma\left(h\to\tau\tau\to\pi^+\pi^-+2\nu\right)}{d\phi_{CP}}\propto 1-\frac{\pi^2}{16}\cos\left(\phi_{CP}-2\phi\right)$$

- It is experimentally challenging because the neutrinos are not reconstructed

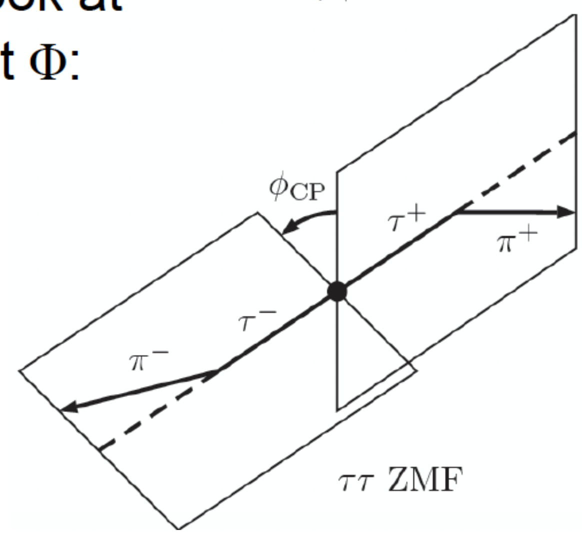

CP test in H→ττ decay

- There are two methods to extract CP from H→ττ decay:

  Impact Parameter (IP) method:
  - Approximately reconstruct the tau decay plane from its leading track and IP
  - Best for the $\tau\to\pi\nu$ decay. The analyzing power is compromised for other tau decays

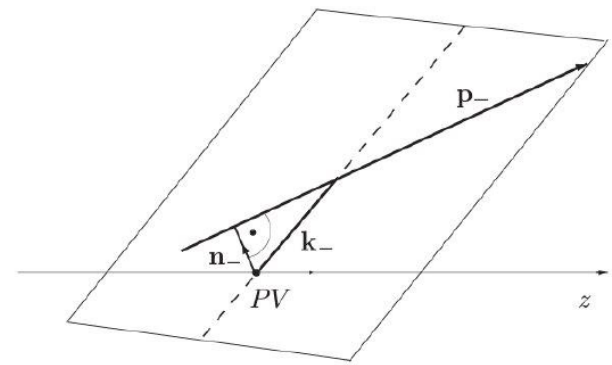

  Using the $\tau\to\rho\nu\to\pi^{\pm}\pi^{0}\nu$ decay:
  - The tau decay plane can be approximately reconstructed by the track and neutral pion
  - However, the relative energy of $\pi^{\pm}$, π^{0} need to be classified in order to maximize the analyzing power

Phys. Rev. D92, 096012

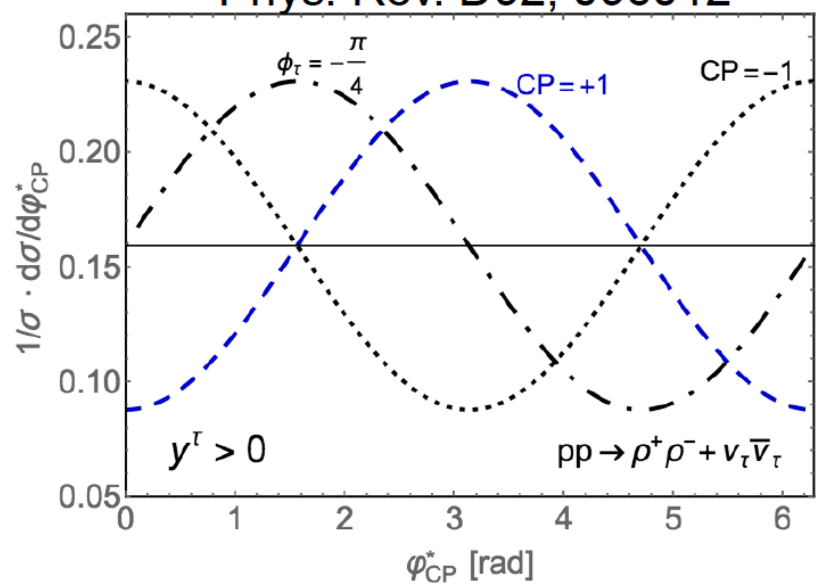

- In order to use the two methods, the tau decay modes (substructure) need to be well differenciated (next few slides)

A few extra references:
EPJC 74 (2014) 3164, Phys. Rev. D88 076009,
Phys. Lett. B579 (2004) 157, Phys. Lett. B543 (2002) 227

The results from the most sensitive channels are weighted and combined into a plot of ϕ_{CP}

Each BDT/NN score window is weighted by A*S/(S+B), being A the "average asymmetry":

$$A = \frac{1}{N_{bins}} \sum^{N_{bins}} \frac{|CP^{even} - CP^{odd}|}{|CP^{even} + CP^{odd}|}$$

Background is subtracted from data.
(Grey band: unc. on subtracted bkg.)

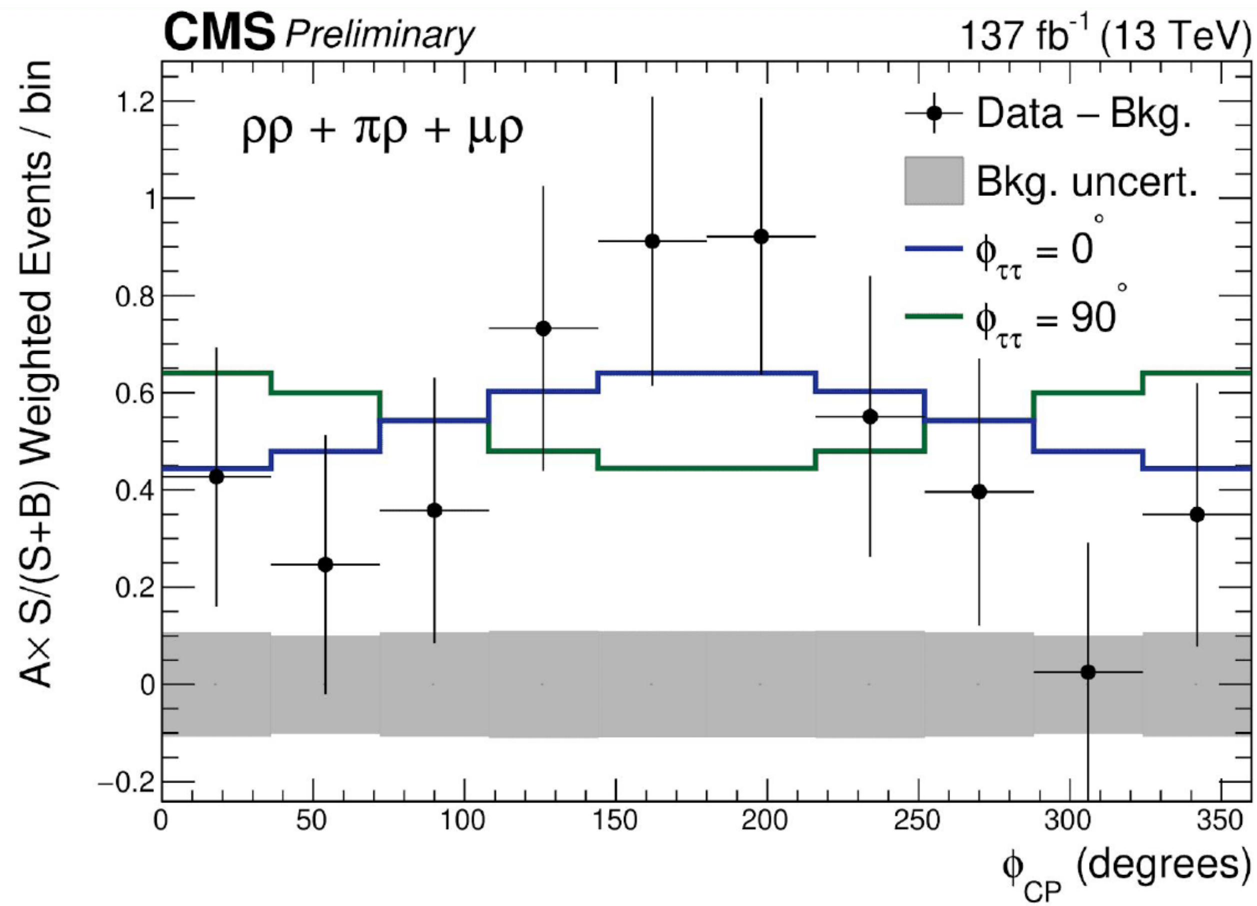

$H \rightarrow \tau\tau$ decays consistent with SM.
CP-even case preferred over CP-odd case with 3.2σ (2.3σ expected).

ggH+2 jets with H→WW*→eνμν

Table 3: Event selection criteria used to define the signal regions for the ggF + 2 jets and VBF event categories.

	ggF + 2 jets	VBF
Preselection	Two isolated, different-flavour leptons ($\ell = e, \mu$) with opposite charge $p_T^{\text{lead}} > 22$ GeV, $p_T^{\text{sublead}} > 15$ GeV $m_{\ell\ell} > 10$ GeV $N_{\text{jet}} \geq 2$	
Background rejection	$N_{b-\text{jet},(p_T>20\text{ GeV})} = 0$ $m_{\tau\tau} < 66$ GeV	
	$\Delta R_{jj} > 1.0$ $p_{T,\ell\ell} > 20$ GeV $m_{\ell\ell} < 90$ GeV $m_T < 150$ GeV	central jet veto outside lepton veto
BDT input variables	$m_{\ell\ell}$, m_T, $p_{T,\ell\ell}$, $\Delta\phi_{\ell\ell}$ $\min \Delta R(\ell_1, j_i)$, $\min \Delta R(\ell_2, j_i)$	m_{jj}, ΔY_{jj}, $m_{\ell\ell}$, m_T, $\Delta\phi_{\ell\ell}$ $\sum_\ell C_\ell$, $\sum_{\ell,j} m_{\ell,j}$, p_T^{tot}

Control region	ggF + 2 jets	VBF
top CR	$N_{b-\text{jet},(p_T>30\text{ GeV})} = 1$	$N_{b-\text{jet},(p_T>20\text{ GeV})} = 1$
$Z \to \tau\tau$ CR	$\lvert m_{\tau\tau} - m_Z \rvert \leq 25$ GeV	
	$p_{T,\ell\ell}$ requirement is omitted	$m_{\ell\ell} < 80$ GeV
WW CR	$m_{\ell\ell} > 90$ GeV m_T requirement is omitted	—-

ggH+2 jets with H→WW*→eνμν

Table 7: Breakdown of the main contributions to the total uncertainty on $\kappa_{Agg}/\kappa_{Hgg}$ based on the fit that exploits both shape and rate information. Individual sources of systematic uncertainty are grouped into either the theoretical or the experimental uncertainty. The sum in quadrature of the individual components differs from the total uncertainty due to correlations between the components.

Source	$\Delta\left(\kappa_{Agg}/\kappa_{Hgg}\right)$
Total data statistical uncertainty	0.4
SR statistical uncertainty	0.33
CR statistical uncertainty	0.10
MC statistical uncertainty	0.14
Total systematic uncertainty	0.28
Theoretical uncertainty	0.23
Top quark bkg.	0.15
ggF signal	0.14
WZ, ZZ, $W\gamma$, $Z\gamma$ bkg.	0.06
WW bkg.	0.06
Z/γ^* bkg.	0.016
VBF bkg.	0.015
Experimental uncertainty	0.21
b-tagging	0.16
Modelling of pile-up	0.10
Jets	0.07
Misidentified leptons	0.04
Luminosity	0.034
Total	0.5

ggH+2 jets with H→WW*→eνμν

CP-even coupling strength scale factor

CP-odd coupling strength scale factor

$$\mathcal{L}_0^{\text{loop}} = -\frac{1}{4}\left(\kappa_{Hgg} g_{Hgg} G^a_{\mu\nu} G^{a,\mu\nu} + \kappa_{Agg} g_{Hgg} G^a_{\mu\nu} \tilde{G}^{a,\mu\nu}\right) H$$

$$\mathcal{L}_0^{\text{loop}} = -\frac{1}{4}\left(\kappa_{gg}\cos(\alpha) g_{Hgg} G^a_{\mu\nu} G^{a,\mu\nu} + \kappa_{gg}\sin(\alpha) g_{Hgg} G^a_{\mu\nu} \tilde{G}^{a,\mu\nu}\right) H$$

Table 6: Post-fit event yields in the signal and control regions obtained from the study of the signal strength parameter $\mu^{\text{ggF+2jets}}$. The quoted uncertainties include the theoretical and experimental systematic sources and those due to sample statistics.

Process	Top CR	WW CR	$Z\to\tau\tau$ CR	SR
ggF + 2 jets	20 ± 20	< 0.1	10 ± 10	60 ± 80
ggF + 0/1 jets	4 ± 1	< 0.1	3 ± 1	40 ± 20
VBF	8 ± 1	< 0.1	7 ± 1	70 ± 10
Other Higgs	6.0 ± 0.3	2.4 ± 0.1	20 ± 4	26 ± 1
$WZ, ZZ, W\gamma, Z\gamma$	40 ± 30	100 ± 30	120 ± 50	240 ± 80
$t\bar{t}, Wt$	17800 ± 200	3100 ± 500	390 ± 60	2300 ± 300
W + jets	600 ± 200	140 ± 30	90 ± 20	390 ± 80
WW	180 ± 80	1400 ± 500	200 ± 70	1200 ± 400
Z + jets	220 ± 30	16 ± 3	1960 ± 70	1000 ± 100
Observed	18886	4778	2800	5209

VBF H→WW*→(eνμν): polarisation measurement in HVV

ATLAS-CONF-2020-055

Higgs boson produced through vector boson fusion (VBF)
- HVV vertex present in production and decay
- access to Higgs coupling to long. and transv. polarized W and Z bosons
- effective lagrangian given by:

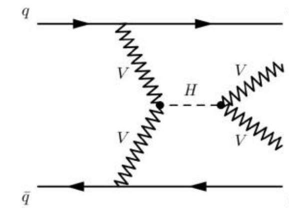

$$\mathcal{L} = \boxed{\kappa_{VV}\left(\frac{2m_W^2}{v}HW_\mu^+W^{-\mu} + \frac{m_Z^2}{v}HZ_\mu Z^\mu\right)} - \boxed{\frac{\varepsilon_{VV}}{2v}\left(2HW_{\mu\nu}^+W^{-\mu\nu} + HZ_{\mu\nu}Z^{\mu\nu} + HA_{\mu\nu}A^{\mu\nu}\right)}$$

SM BSM

with $\kappa_{VV} \simeq a_L$,

$\varepsilon_{VV} \simeq 0.5 \cdot (a_T - a_L)$

$$a_L = \frac{g_{HV_LV_L}}{g_{HVV}}, \quad a_T = \frac{g_{HV_TV_T}}{g_{HVV}}$$

SM: $a_L = a_T = 1$

Optimal discriminant for CP: $\Delta\phi_{jj}$

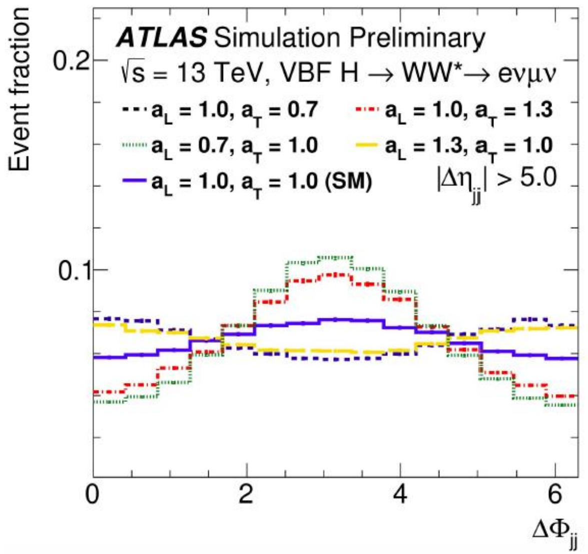

$a_L = 0.90 \pm 0.12$ (stat.) ± 0.14 (syst.)
$a_T = 1.18 \pm 0.29$ (stat.) ± 0.15 (syst.)

Analysis strategy

- Veto central jets and leptons within the rapidity gap spanned by the two leading jets (VBF)
- Dedicated CRs to constrain norm. main bkgs (top, Z+jets)
- BDTs to further separate signal from background

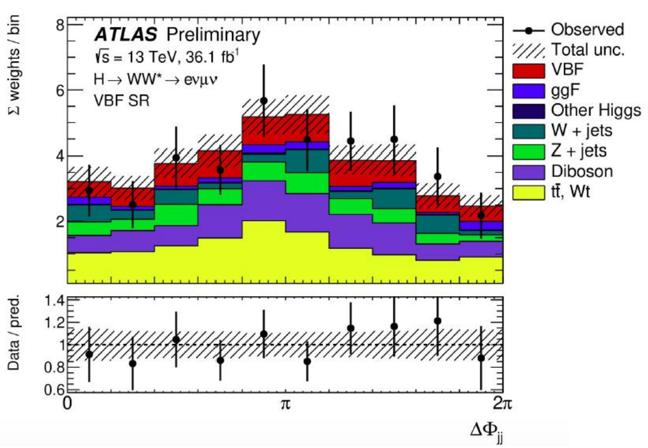

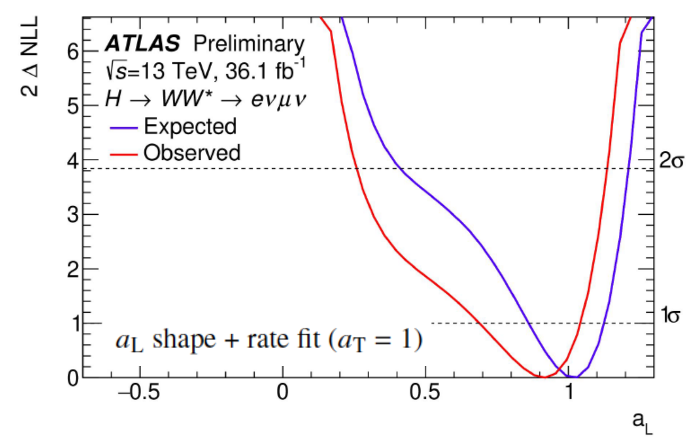

CP parametrisations to probe HVV and Hgg couplings

ATLAS parametrisation

- Lagrangian in Higgs characterisation framework

$$\mathcal{L}_{eff} = H\left\{c_\alpha \kappa_{SM}\left[\frac{1}{2}\frac{2m_V^2}{v}Z_\mu Z^\mu + g_{HWW}W_\mu W^\mu\right] - \frac{1}{4}\frac{1}{\Lambda}s_\alpha \kappa_{AZZ}Z_{\mu\nu}\tilde{Z}^{\mu\nu} - \frac{1}{2}\frac{1}{\Lambda}s_\alpha \kappa_{AWW}W^+_{\mu\nu}\tilde{W}^{-\mu\nu}\right\}$$

$$\mathcal{L}_0^{\text{loop}} = -\frac{1}{4}\left(\kappa_{Hgg}g_{Hgg}G^a_{\mu\nu}G^{a,\mu\nu} + \kappa_{Agg}g_{Hgg}G^a_{\mu\nu}\tilde{G}^{a,\mu\nu}\right)H,$$

- $\boldsymbol{k_{AVV}/k_{HVV}}$ or similar extracted from the fit
- Other parametrisation in VBF $H\rightarrow\tau\tau$ which has CP-odd contribution parametrised by $\tilde{d}$

$$\tilde{d} = \frac{1}{4}\frac{v}{\Lambda}\frac{k_{AVV}}{k_{SM}}\tan\alpha$$

CMS parametrisation

Scattering amplitude:

$$A(\text{HVV}) = \frac{1}{v}\left[a_1^{\text{VV}} + \frac{\kappa_1^{\text{VV}}q_{\text{V1}}^2 + \kappa_2^{\text{VV}}q_{\text{V2}}^2}{\left(\Lambda_1^{\text{VV}}\right)^2} + \frac{\kappa_3^{\text{VV}}(q_{\text{V1}}+q_{\text{V2}})^2}{\left(\Lambda_Q^{\text{VV}}\right)^2}\right] m_{\text{V1}}^2\epsilon_{\text{V1}}^*\epsilon_{\text{V2}}^* + \frac{1}{v}a_2^{\text{VV}}f_{\mu\nu}^{*(1)}f^{*(2),\mu\nu} + \frac{1}{v}a_3^{\text{VV}}f_{\mu\nu}^{*(1)}\tilde{f}^{*(2),\mu\nu},$$

f_{a3} parameter extracted from the fit (ratio of cross sections)

$$f_{a3}^{\text{ggH}} = \frac{|a_3^{\text{gg}}|^2}{|a_2^{\text{gg}}|^2 + |a_3^{\text{gg}}|^2}\,\text{sign}\left(\frac{a_3^{\text{gg}}}{a_2^{\text{gg}}}\right).$$

Alessia Murrone slides SM@LHC 2021

H→4l to probe HVV, Hgg and Htt couplings

arXiv:2104.12152

Table 2: The numbers of events expected in the SM for different H signal (sig) and background (bkg) contributions and the observed number of events in each category defined in Scheme 1 targeting Hff and Hgg anomalous couplings. The $t\bar{t}H$ signal expectation is quoted for the SM and anomalous coupling ($\kappa_t = 0$, $\tilde{\kappa}_t = 1.6$) scenario, both generated with the same cross section.

	Untagged	VBF-1jet	VBF-2jet	VH-leptonic	VH-hadronic	$t\bar{t}H$-leptonic	$t\bar{t}H$-hadronic
ggH sig	182.98	15.50	6.70	0.35	4.68	0.02	0.18
VBF sig	7.23	3.28	7.23	0.05	0.28	0.01	0.05
WH sig	2.68	0.22	0.22	1.07	1.17	0.03	0.03
ZH sig	2.20	0.14	0.15	0.26	0.78	0.02	0.05
$b\bar{b}H$ sig	1.90	0.13	0.08	0.03	0.07	0.00	0.01
$t\bar{t}H$ sig	0.43	0.00	0.08	0.14	0.15	0.68	0.86
($\tilde{\kappa}_t = 1.6$)	(0.45)	(0.00)	(0.12)	(0.15)	(0.15)	(0.87)	(1.18)
tH sig	0.14	0.01	0.10	0.04	0.03	0.04	0.03
Signal	197.89	19.31	14.57	2.00	7.40	0.80	1.23
$q\bar{q} \to 4\ell$ bkg	210.50	6.93	1.92	2.23	1.87	0.08	0.04
$gg \to 4\ell$ bkg	19.79	1.53	0.56	0.38	0.24	0.01	0.01
EW bkg	3.43	0.18	1.37	0.26	0.57	0.24	1.07
$Z + X$ bkg	77.94	2.46	4.88	1.20	3.29	0.21	1.07
Total	509.55	30.41	23.30	6.05	13.38	1.33	3.41
Observed	539	27	20	10	12	0	2

H→4l to probe HVV, Hgg and Htt couplings

arXiv:2104.12152

Table 3: The numbers of events expected in the SM for different H signal (sig) and background (bkg) contributions and the observed number of events in each category defined in Scheme 2 targeting HVV anomalous couplings. The EW (VBF, WH, and ZH) signal expectation is quoted for the SM and four anomalous coupling ($a_3/a_2/\kappa_1/\kappa_2^{Z\gamma}$) scenarios $f_{ai} = 1$, all generated with the same total EW production cross section.

	Untagged	Boosted	VBF-1jet	VBF-2jet	VH-leptonic	VH-hadronic
ggH sig	171.46	6.48	15.15	10.44	0.35	5.99
VBF sig	5.06	1.18	2.64	8.60	0.06	0.54
($a_3/a_2/\kappa_1/\kappa_2^{Z\gamma}$)	(0.29/0.29/0.05/0.09)	(0.69/0.54/0.52/0.48)	(0.12/0.09/0.03/0.05)	(6.10/4.95/1.91/1.83)	(0.03/0.02/0.01/0.01)	(0.28/0.21/0.07/0.07)
WH sig	2.18	0.43	0.29	0.22	1.11	1.20
($a_3/a_2/\kappa_1/\kappa_2^{Z\gamma}$)	(1.93/3.15/0.72/0.00)	(3.81/3.20/6.28/0.00)	(0.83/0.92/0.22/0.00)	(1.20/1.05/2.04/0.00)	(2.75/2.86/3.47/0.00)	(3.43/3.33/2.93/0.00)
ZH sig	1.87	0.34	0.16	0.16	0.26	0.79
($a_3/a_2/\kappa_1/\kappa_2^{Z\gamma}$)	(0.99/1.89/0.68/1.17)	(1.87/1.66/4.14/12.34)	(0.30/0.35/0.12/0.27)	(0.56/0.51/1.30/3.88)	(0.42/0.48/0.65/1.82)	(1.42/1.53/1.84/4.69)
$b\bar{b}$H sig	1.84	0.04	0.13	0.09	0.03	0.09
$t\bar{t}$H sig	1.65	0.04	0.00	0.32	0.13	0.19
tH sig	0.13	0.02	0.01	0.12	0.04	0.05
Signal	184.1	8.5	18.4	19.8	1.9	8.8
($a_3/a_2/\kappa_1/\kappa_2^{Z\gamma}$)	(178.2/180.3/176.4/176.2)	(12.9/12.0/17.5/19.4)	(16.5/16.7/15.7/15.6)	(18.7/17.4/16.1/16.6)	(3.7/3.9/4.6/2.3)	(11.4/11.4/11.1/11.0)
$q\bar{q} \to 4\ell$ bkg	206.05	1.89	6.78	2.78	2.21	2.30
$gg \to 4\ell$ bkg	19.05	0.38	1.52	0.76	0.37	0.31
EW bkg	3.50	0.66	0.20	1.98	0.23	0.85
Z + X bkg	69.87	3.73	2.46	9.70	1.20	4.10
Total	481.3	15.1	29.3	34.9	5.9	16.24
($a_3/a_2/\kappa_1/\kappa_2^{Z\gamma}$)	(475.4/477.5/473.6/473.4)	(19.5/18.6/24.1/26.0)	(27.4/27.6/26.6/26.5)	(33.8/32.4/31.1/31.6)	(7.7/7.9/8.6/6.3)	(18.83/18.78/18.54/18.47)
Observed	512	18	27	30	10	13

H→4l to probe HVV, Hgg and Htt couplings

arXiv:2104.12152

Table 4: The list of kinematic observables used for category selection and fitting in categorization Schemes 1 and 2. Only the main features involving the kinematic discriminants in the category selection are listed, while complete details are given in Section 3. The Untagged category includes the events not selected in the other categories.

Category	Selection	Observables $\vec{x}$ for fitting
Scheme 1		
VBF-1jet	$\mathcal{D}_{\text{1jet}}^{\text{VBF}} > 0.7$	$\mathcal{D}_{\text{bkg}}$
VBF-2jet	$\mathcal{D}_{\text{2jet}}^{\text{VBF}} > 0.5$	$\mathcal{D}_{\text{bkg}}, \mathcal{D}_{\text{2jet}}^{\text{VBF}}, \mathcal{D}_{0-}^{\text{ggH}}, \mathcal{D}_{\text{CP}}^{\text{ggH}}$
VH-hadronic	$\mathcal{D}_{\text{2jet}}^{\text{VH}} > 0.5$	$\mathcal{D}_{\text{bkg}}$
VH-leptonic	see Section 3	$\mathcal{D}_{\text{bkg}}$
$\mathrm{t\bar{t}H}$-hadronic	see Section 3	$\mathcal{D}_{\text{bkg}}, \mathcal{D}_{0-}^{\mathrm{t\bar{t}H}}$
$\mathrm{t\bar{t}H}$-leptonic	see Section 3	$\mathcal{D}_{\text{bkg}}, \mathcal{D}_{0-}^{\mathrm{t\bar{t}H}}$
Untagged	none of the above	$\mathcal{D}_{\text{bkg}}$
Scheme 2		
Boosted	$p_{\mathrm{T}}^{4\ell} > 120\,\text{GeV}$	$\mathcal{D}_{\text{bkg}}, p_{\mathrm{T}}^{4\ell}$
VBF-1jet	$\mathcal{D}_{\text{1jet}}^{\text{VBF}} > 0.7$	$\mathcal{D}_{\text{bkg}}, p_{\mathrm{T}}^{4\ell}$
VBF-2jet	$\mathcal{D}_{\text{2jet}}^{\text{VBF}} > 0.5$	$\mathcal{D}_{\text{bkg}}^{\text{EW}}, \mathcal{D}_{0h+}^{\text{VBF+dec}}, \mathcal{D}_{0-}^{\text{VBF+dec}}, \mathcal{D}_{\Lambda1}^{\text{VBF+dec}}, \mathcal{D}_{\Lambda1}^{Z\gamma,\text{VBF+dec}}, \mathcal{D}_{\text{int}}^{\text{VBF}}, \mathcal{D}_{\text{CP}}^{\text{VBF}}$
VH-hadronic	$\mathcal{D}_{\text{2jet}}^{\text{VH}} > 0.5$	$\mathcal{D}_{\text{bkg}}^{\text{EW}}, \mathcal{D}_{0h+}^{\text{VH+dec}}, \mathcal{D}_{0-}^{\text{VH+dec}}, \mathcal{D}_{\Lambda1}^{\text{VH+dec}}, \mathcal{D}_{\Lambda1}^{Z\gamma,\text{VH+dec}}, \mathcal{D}_{\text{int}}^{\text{VH}}, \mathcal{D}_{\text{CP}}^{\text{VH}}$
VH-leptonic	see Section 3	$\mathcal{D}_{\text{bkg}}, p_{\mathrm{T}}^{4\ell}$
Untagged	none of the above	$\mathcal{D}_{\text{bkg}}, \mathcal{D}_{0h+}^{\text{dec}}, \mathcal{D}_{0-}^{\text{dec}}, \mathcal{D}_{\Lambda1}^{\text{dec}}, \mathcal{D}_{\Lambda1}^{Z\gamma,\text{dec}}, \mathcal{D}_{\text{int}}^{\text{dec}}, \mathcal{D}_{\text{CP}}^{\text{dec}}$

H→4l to probe HVV, Hgg and Htt couplings

General Lorentz invariant form of **HVV scattering amplitude :**

$$A(\mathrm{HVV}) = \frac{1}{v}\left[a_1^{\mathrm{VV}} + \frac{\kappa_1^{\mathrm{VV}} q_{\mathrm{V1}}^2 + \kappa_2^{\mathrm{VV}} q_{\mathrm{V2}}^2}{\left(\Lambda_1^{\mathrm{VV}}\right)^2} + \frac{\kappa_3^{\mathrm{VV}}(q_{\mathrm{V1}}+q_{\mathrm{V2}})^2}{\left(\Lambda_Q^{\mathrm{VV}}\right)^2}\right] m_{\mathrm{V1}}^2 \epsilon_{\mathrm{V1}}^* \epsilon_{\mathrm{V2}}^* + \frac{1}{v} a_2^{\mathrm{VV}} f_{\mu\nu}^{*(1)} f^{*(2),\mu\nu} + \frac{1}{v} a_3^{\mathrm{VV}} f_{\mu\nu}^{*(1)} \tilde{f}^{*(2),\mu\nu},$$

SU(2)xU(1) enforces relations between ZZ,WW,$\gamma\gamma$ and Zγ couplings :

$$\begin{aligned}
a_1^{\mathrm{WW}} &= a_1^{\mathrm{ZZ}}, \\
a_2^{\mathrm{WW}} &= c_w^2 a_2^{\mathrm{ZZ}} + s_w^2 \cancel{a_2^{\gamma\gamma}} + 2 s_w c_w \cancel{a_2^{\mathrm{Z}\gamma}}, \\
a_3^{\mathrm{WW}} &= c_w^2 a_3^{\mathrm{ZZ}} + s_w^2 \cancel{a_3^{\gamma\gamma}} + 2 s_w c_w \cancel{a_3^{\mathrm{Z}\gamma}}, \\
\frac{\kappa_1^{\mathrm{WW}}}{(\Lambda_1^{\mathrm{WW}})^2}(c_w^2 - s_w^2) &= \frac{\kappa_1^{\mathrm{ZZ}}}{(\Lambda_1^{\mathrm{ZZ}})^2} + 2 s_w^2 \frac{\cancel{a_2^{\gamma\gamma}} - a_2^{\mathrm{ZZ}}}{m_{\mathrm{Z}}^2} + 2\frac{s_w}{c_w}(c_w^2 - s_w^2)\frac{\cancel{a_2^{\mathrm{Z}\gamma}}}{m_{\mathrm{Z}}^2}, \\
\frac{\kappa_2^{\mathrm{Z}\gamma}}{(\Lambda_1^{\mathrm{Z}\gamma})^2}(c_w^2 - s_w^2) &= 2 s_w c_w \left(\frac{\kappa_1^{\mathrm{ZZ}}}{(\Lambda_1^{\mathrm{ZZ}})^2} + \frac{\cancel{a_2^{\gamma\gamma}} - a_2^{\mathrm{ZZ}}}{m_{\mathrm{Z}}^2}\right) + 2(c_w^2 - s_w^2)\frac{\cancel{a_2^{\mathrm{Z}\gamma}}}{m_{\mathrm{Z}}^2}
\end{aligned}$$

Assume $a^{\gamma\gamma}$ and $a^{Z\gamma}$ constrained by H→ $\gamma\gamma$ and H→Zγ measurements

4 independent couplings : a_1 (SM), a_2, a_3 (CP-Odd), k_1

arXiv:2104.12152

Summary of anomalous Htt, Hgg and HVV couplings:

Parameter	Scenario	Observed	Expected
f_{a3}^{ggH}	ggH ($H \to 4\ell$)	$-0.04^{+1.04}_{-0.96}$ $[-1, 1]$	0 ± 1 $[-1, 1]$
f_{CP}^{Htt}	tH & $t\bar{t}$H ($H \to 4\ell$)	$\pm(0.88^{+0.12}_{-1.88})$ $[-1, 1]$	0 ± 1 $[-1, 1]$
	tH & $t\bar{t}$H ($H \to \gamma\gamma$) [26]	0.00 ± 0.33 $[-0.67, 0.67]$	0.00 ± 0.49 $[-0.82, 0.82]$
	tH & $t\bar{t}$H ($H \to 4\ell$ & $\gamma\gamma$)	0.00 ± 0.33 $[-0.67, 0.67]$	0.00 ± 0.48 $[-0.81, 0.81]$
	ggH ($H \to 4\ell$)	$-0.01^{+1.01}_{-0.99}$ $[-1, 1]$	0 ± 1 $[-1, 1]$
	ggH & tH & $t\bar{t}$H ($H \to 4\ell$)	$-0.56^{+1.56}_{-0.44}$ $[-1, 1]$	0.00 ± 0.47 $[-1, 1]$
	ggH & tH & $t\bar{t}$H ($H \to 4\ell$ & $\gamma\gamma$)	$-0.04^{+0.38}_{-0.36}$ $[-0.69, 0.68]$	0.00 ± 0.30 $[-0.70, 0.70]$

Parameter	Scenario		Observed	Expected
f_{a3}	Approach 1	best fit	0.00004	0.00000
	$f_{a2} = f_{\Lambda 1} = f_{\Lambda 1}^{Z\gamma} = 0$	68% CL	$[-0.00007, 0.00044]$	$[-0.00081, 0.00081]$
		95% CL	$[-0.00055, 0.00168]$	$[-0.00412, 0.00412]$
	Approach 1	best fit	-0.00805	0.00000
	float $f_{a2}, f_{\Lambda 1}, f_{\Lambda 1}^{Z\gamma}$	68% CL	$[-0.02656, 0.00034]$	$[-0.00086, 0.00086]$
		95% CL	$[-0.07191, 0.00990]$	$[-0.00423, 0.00422]$
	Approach 2	best fit	0.00005	0.0000
	float $f_{a2}, f_{\Lambda 1}$	68% CL	$[-0.00010, 0.00061]$	$[-0.0012, 0.0012]$
		95% CL	$[-0.00072, 0.00218]$	$[-0.0057, 0.0057]$

Summary of constraints on the Htt, Hgg and HVV couplings in the **Higgs basis of SMEFT:**

Channels	Coupling	Observed	Expected	Observed correlation			
				c_{gg}	$\tilde{c}_{gg}$	κ_t	$\tilde{\kappa}_t$
tH & $t\bar{t}$H & ggH	c_{gg}	$-0.0012^{+0.0022}_{-0.0174}$	$0.0000^{+0.0019}_{-0.0196}$	1	-0.050	-0.941	$+0.029$
	$\tilde{c}_{gg}$	$-0.0017^{+0.0160}_{-0.0130}$	$0.0000^{+0.0138}_{-0.0138}$		1	$+0.046$	-0.568
	κ_t	$1.05^{+0.25}_{-0.20}$	$1.00^{+0.34}_{-0.26}$			1	$+0.168$
	$\tilde{\kappa}_t$	$-0.01^{+0.69}_{-0.67}$	$0.00^{+0.71}_{-0.71}$				1
				δc_z	c_{zz}	$c_{z\Box}$	$\tilde{c}_{zz}$
VBF & VH & $H \to 4\ell$	δc_z	$-0.03^{+0.06}_{-0.25}$	$0.00^{+0.07}_{-0.27}$	1	$+0.241$	-0.060	-0.009
	c_{zz}	$0.01^{+0.11}_{-0.10}$	$0.00^{+0.22}_{-0.16}$		1	-0.884	$+0.058$
	$c_{z\Box}$	$-0.02^{+0.04}_{-0.04}$	$0.00^{+0.06}_{-0.09}$			1	$+0.020$
	$\tilde{c}_{zz}$	$-0.11^{+0.30}_{-0.31}$	$0.00^{+0.63}_{-0.63}$				1

$ttH(\gamma\gamma + 4l)$

H→4l to probe HVV, Hgg and Htt couplings

arXiv:2104.12152

Category	Selection	Observables $\vec{x}$ for fitting
Scheme 1		
VBF-1jet	$\mathcal{D}^{\mathrm{VBF}}_{\mathrm{1jet}} > 0.7$	$\mathcal{D}_{\mathrm{bkg}}$
VBF-2jet	$\mathcal{D}^{\mathrm{VBF}}_{\mathrm{2jet}} > 0.5$	$\mathcal{D}_{\mathrm{bkg}}, \mathcal{D}^{\mathrm{VBF}}_{\mathrm{2jet}}, \mathcal{D}^{\mathrm{ggH}}_{0-}, \mathcal{D}^{\mathrm{ggH}}_{\mathrm{CP}}$
VH-hadronic	$\mathcal{D}^{\mathrm{VH}}_{\mathrm{2jet}} > 0.5$	$\mathcal{D}_{\mathrm{bkg}}$
VH-leptonic	see Section $\boxed{3}$	$\mathcal{D}_{\mathrm{bkg}}$
$\mathrm{t\bar{t}H}$-hadronic	see Section $\boxed{3}$	$\mathcal{D}_{\mathrm{bkg}}, \mathcal{D}^{\mathrm{t\bar{t}H}}_{0-}$
$\mathrm{t\bar{t}H}$-leptonic	see Section $\boxed{3}$	$\mathcal{D}_{\mathrm{bkg}}, \mathcal{D}^{\mathrm{t\bar{t}H}}_{0-}$
Untagged	none of the above	$\mathcal{D}_{\mathrm{bkg}}$
Scheme 2		
Boosted	$p_{\mathrm{T}}^{4\ell} > 120\,\mathrm{GeV}$	$\mathcal{D}_{\mathrm{bkg}}, p_{\mathrm{T}}^{4\ell}$
VBF-1jet	$\mathcal{D}^{\mathrm{VBF}}_{\mathrm{1jet}} > 0.7$	$\mathcal{D}_{\mathrm{bkg}}, p_{\mathrm{T}}^{4\ell}$
VBF-2jet	$\mathcal{D}^{\mathrm{VBF}}_{\mathrm{2jet}} > 0.5$	$\mathcal{D}^{\mathrm{EW}}_{\mathrm{bkg}}, \mathcal{D}^{\mathrm{VBF+dec}}_{0h+}, \mathcal{D}^{\mathrm{VBF+dec}}_{0-}, \mathcal{D}^{\mathrm{VBF+dec}}_{\Lambda1}, \mathcal{D}^{Z\gamma,\mathrm{VBF+dec}}_{\Lambda1}, \mathcal{D}^{\mathrm{VBF}}_{\mathrm{int}}, \mathcal{D}^{\mathrm{VBF}}_{\mathrm{CP}}$
VH-hadronic	$\mathcal{D}^{\mathrm{VH}}_{\mathrm{2jet}} > 0.5$	$\mathcal{D}^{\mathrm{EW}}_{\mathrm{bkg}}, \mathcal{D}^{\mathrm{VH+dec}}_{0h+}, \mathcal{D}^{\mathrm{VH+dec}}_{0-}, \mathcal{D}^{\mathrm{VH+dec}}_{\Lambda1}, \mathcal{D}^{Z\gamma,\mathrm{VH+dec}}_{\Lambda1}, \mathcal{D}^{\mathrm{VH}}_{\mathrm{int}}, \mathcal{D}^{\mathrm{VH}}_{\mathrm{CP}}$
VH-leptonic	see Section $\boxed{3}$	$\mathcal{D}_{\mathrm{bkg}}, p_{\mathrm{T}}^{4\ell}$
Untagged	none of the above	$\mathcal{D}_{\mathrm{bkg}}, \mathcal{D}^{\mathrm{dec}}_{0h+}, \mathcal{D}^{\mathrm{dec}}_{0-}, \mathcal{D}^{\mathrm{dec}}_{\Lambda1}, \mathcal{D}^{Z\gamma,\mathrm{dec}}_{\Lambda1}, \mathcal{D}^{\mathrm{dec}}_{\mathrm{int}}, \mathcal{D}^{\mathrm{dec}}_{\mathrm{CP}}$

ttH: ME based discriminants from MELA

- JHUGen generated LO and NLO events
- The MEs use the 4-momentum of tt->(ff'b,ff'b) and H
- small impact from LO/NLO and PDF scale variation

$$\mathcal{D}_{0-} = \frac{\mathcal{P}_{0+}(\vec{\Omega})}{\mathcal{P}_{0+}(\vec{\Omega}) + \mathcal{P}_{0-}(\vec{\Omega})},$$

for 0+ vs 0-

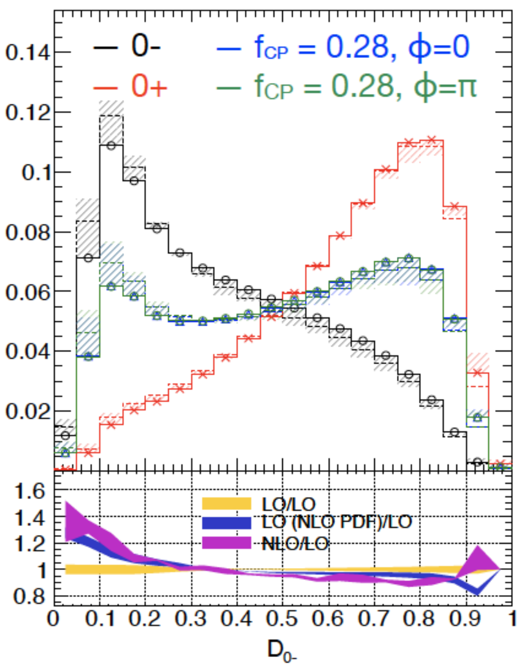

$$\mathcal{D}_{CP} = \frac{\mathcal{P}_{\rm int}(\vec{\Omega})}{\mathcal{P}_{0+}(\vec{\Omega}) + \mathcal{P}_{0-}(\vec{\Omega})},$$

for CP mixture, ϕ=0

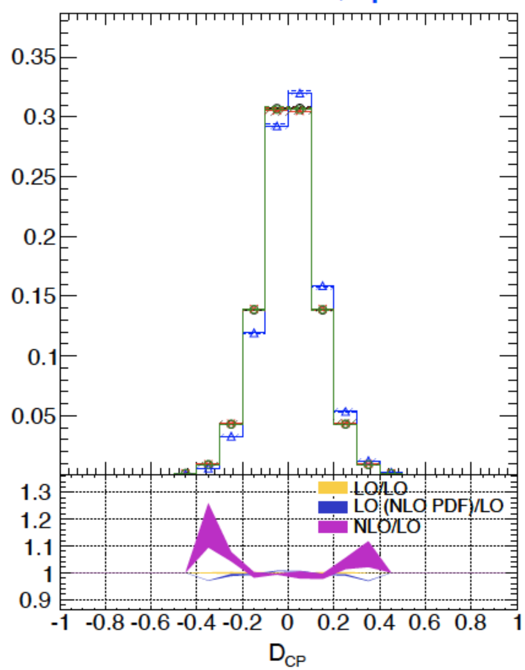

$$\mathcal{D}_{CP}^{\perp} = \frac{\mathcal{P}_{\rm int}^{\perp}(\vec{\Omega})}{\mathcal{P}_{0+}(\vec{\Omega}) + \mathcal{P}_{0-}(\vec{\Omega})},$$

for CP mixture, ϕ=90

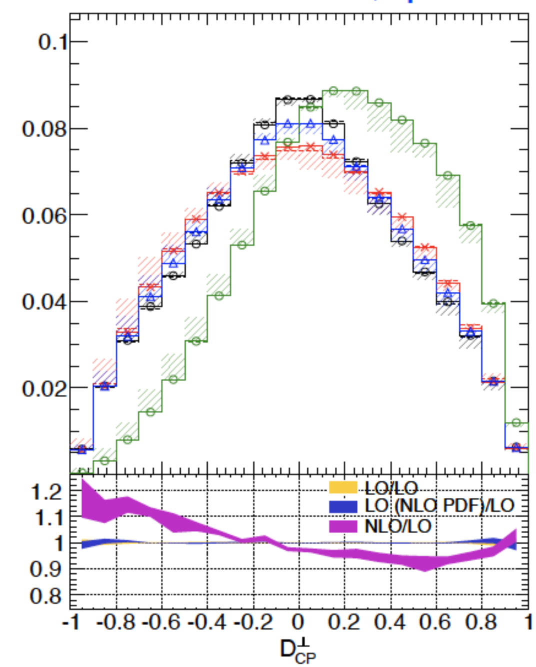

Meng Xiao @ ICHEP2020

tqH process

- t-channel + s-channel
- Strong Hff and HVV interference
- Sensitive to the size, sign and CP of the Hff coupling

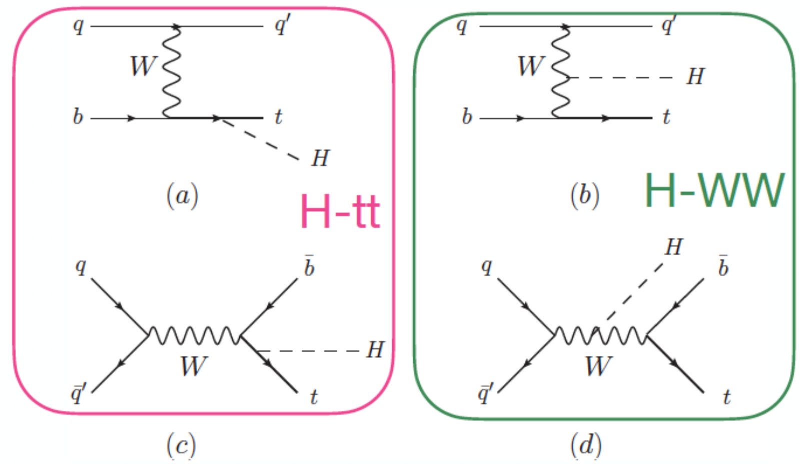

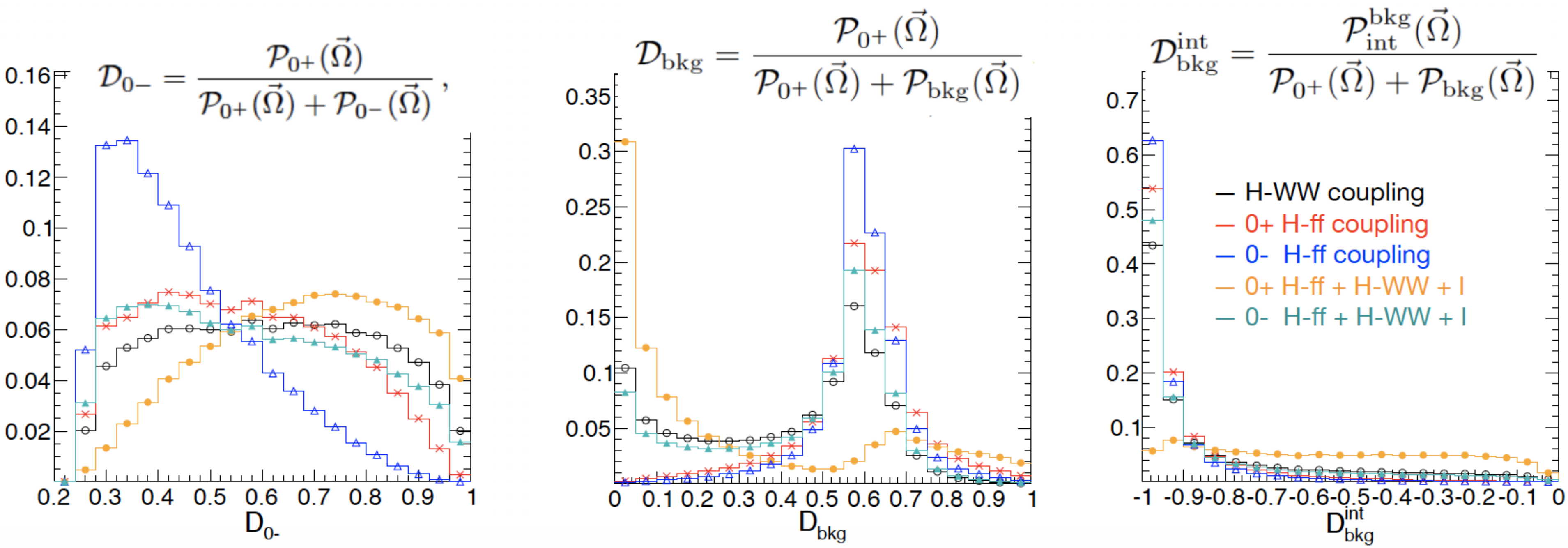

Meng Xiao @ ICHEP2020

Reinterpretations cross-sections measurements in H→γγ

ATLAS-CONF-2019-029

- Limits on single c_i assuming $c_{j\neq i} = 0$
- No deviation from SM observed
- Not taking event rate into account reduces sensitivity to CP-odd Wilson coefficients
- But makes test of CP violation less model-dependent

\- Better constraints when including quadratic terms

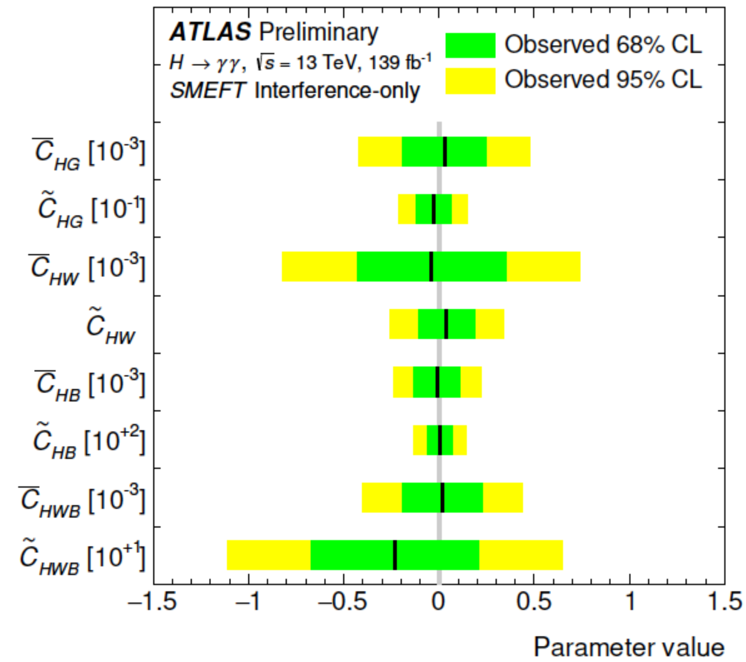

Coefficient	95% CL, interference-only terms	95% CL, interference and quadratic terms
$\overline{C}_{HG}$	$[-4.2, 4.8] \times 10^{-4}$	$[-6.1, 4.7] \times 10^{-4}$
$\tilde{C}_{HG}$	$[-2.1, 1.6] \times 10^{-2}$	$[-1.5, 1.4] \times 10^{-3}$
$\overline{C}_{HW}$	$[-8, 2, 7.4] \times 10^{-4}$	$[-8.3, 8.3] \times 10^{-4}$
$\tilde{C}_{HW}$	$[-0.26, 0.33]$	$[-3.7, 3.7] \times 10^{-3}$
$\overline{C}_{HB}$	$[-2.4, 2.3] \times 10^{-4}$	$[-2.4, 2.4] \times 10^{-4}$
$\tilde{C}_{HB}$	$[-13.0, 14.0]$	$[-1.2, 1.1] \times 10^{-3}$
$\overline{C}_{HWB}$	$[-4.0, 4.4] \times 10^{-4}$	$[-4.2, 4.2] \times 10^{-4}$
$\tilde{C}_{HWB}$	$[-11.1, 6.5]$	$[-2.0, 2.0] \times 10^{-3}$

Is the top-Higgs coupling a pure scalar interaction ?

$J^{CP} = 0^{++}$?

Phys.Rev.Lett.125(2020)061802

No deviations found in CP properties of the Higgs couplings to gauge bosons

Caveat: in those, CP-odd contributions enter only via higher-order operators

NEW: pseudoscalar admixture directly tested in top-Higgs interaction using ttH/tH events with H→γγ

$$\mathcal{L}_t = -\frac{m_t}{v}(\kappa_t \bar{t}t + i\tilde{\kappa}_t \bar{t}\gamma_5 t)H$$

CP

SM: $(\kappa_t, \tilde{\kappa}_t) = (1, 0)$

$$\kappa_t = k_t \cos\alpha$$
$$\tilde{\kappa}_t = k_t \sin\alpha$$

CP mixing angle: α

CP-odd contributions would alter:

- rates and kinematics of *ttH* and *tH* processes
  - *tH* also sensitive to the sign of y_t
- loop-induced Higgs couplings to gluons and photons

Rate variation vs. CP mixing angle α

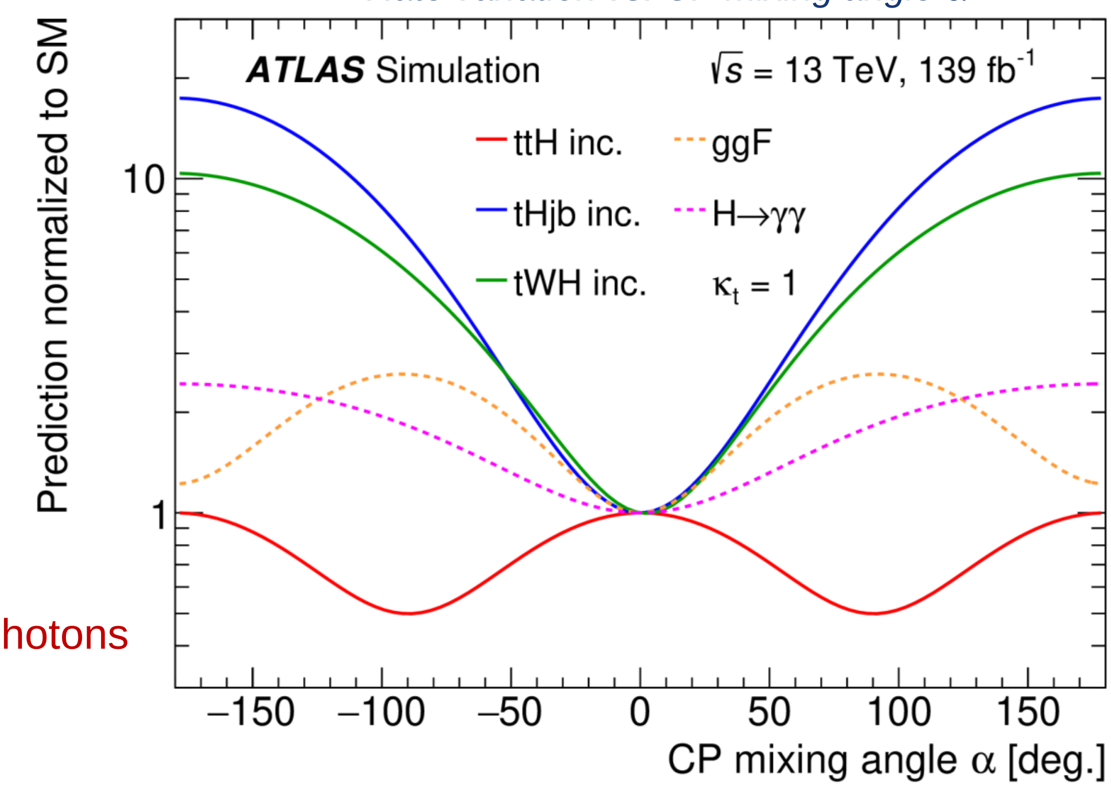

Is the top-Higgs coupling a pure scalar interaction ?

$J^{CP} = 0^{++}$?

Phys.Rev.Lett.125(2020)061802

No deviations found in CP properties of the Higgs couplings to gauge bosons

Caveat: in those, CP-odd contributions enter only via higher-order operators

NEW: pseudoscalar admixture directly tested in top-Higgs interaction using ttH/tH events with H→γγ

$$\mathcal{L}_t = -\frac{m_t}{v}(\kappa_t \bar{t}t + i\tilde{\kappa}_t \bar{t}\gamma_5 t)H$$

$$\text{SM: } (\kappa_t, \tilde{\kappa}_t) = (1,0)$$

$$\kappa_t = k_t \cos\alpha$$
$$\tilde{\kappa}_t = k_t \sin\alpha$$

ATLAS:

1D fit: CP mixing angle α

2D fit: $k_t \cos\alpha$ vs $k_t \sin\alpha$

CMS:

1D fit: $f_{CP}^{Htt} = \frac{|\tilde{\kappa}_t|^2}{|\kappa_t|^2 + |\tilde{\kappa}_t|^2} \mathrm{sign}(\tilde{\kappa}_t/\kappa_t)$

Expected event yields in each analysis region

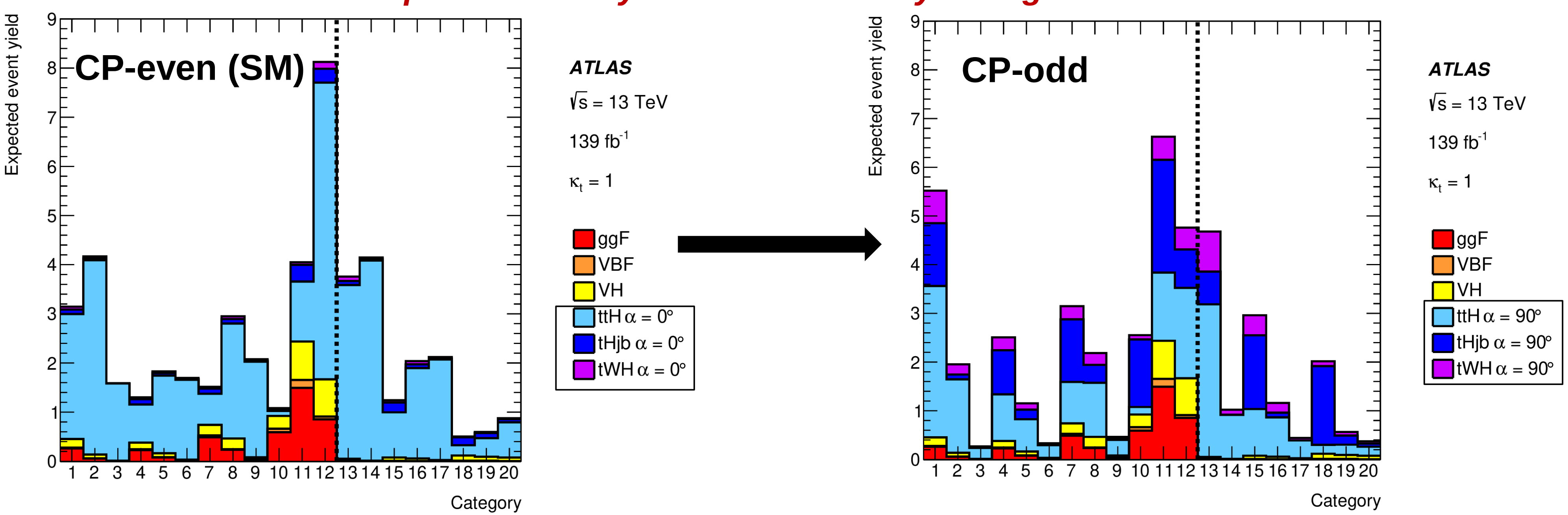

Is the top-Higgs coupling a pure scalar interaction ?

$J^{CP} = 0^{++}$?

No deviations found in CP properties of the Higgs couplings to gauge bosons

Caveat: in those, CP-odd contributions enter only via higher-order operators

NEW: pseudoscalar admixture directly tested in top-Higgs interaction using ttH/tH events with H→γγ

$$\mathcal{L}_t = -\frac{m_t}{v}(\kappa_t \bar{t}t + i\tilde{\kappa}_t \bar{t}\gamma_5 t)H \qquad \text{SM: } (\kappa_t, \tilde{\kappa}_t) = (1, 0) \qquad \begin{aligned} \kappa_t &= k_t \cos\alpha \\ \tilde{\kappa}_t &= k_t \sin\alpha \end{aligned}$$

ATLAS: 1D fit: CP mixing angle α

2D fit: $k_t \cos\alpha$ vs $k_t \sin\alpha$

CMS: 1D fit: $f_{CP}^{Htt} = \frac{|\tilde{\kappa}_t|^2}{|\kappa_t|^2 + |\tilde{\kappa}_t|^2}\,\mathrm{sign}(\tilde{\kappa}_t/\kappa_t)$

Signal parametrisation

signal yields parametrised as function of (k_t, α) or (μ_{ttH}, f_{CP}^{Htt}) CP parameters

Models used

ATLAS:
ttH, tHjb & tWH @NLO
Higgs Characterisation

CMS:
ttH @LO
JHUGEN with MELA

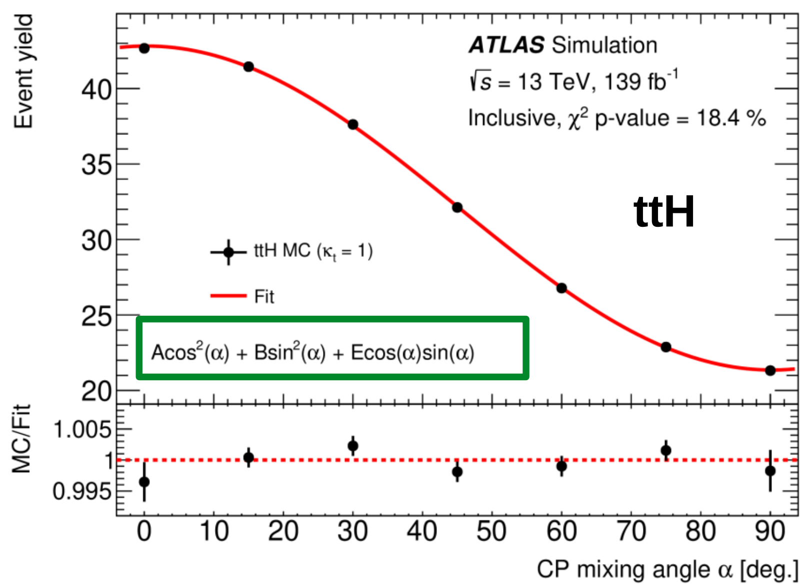

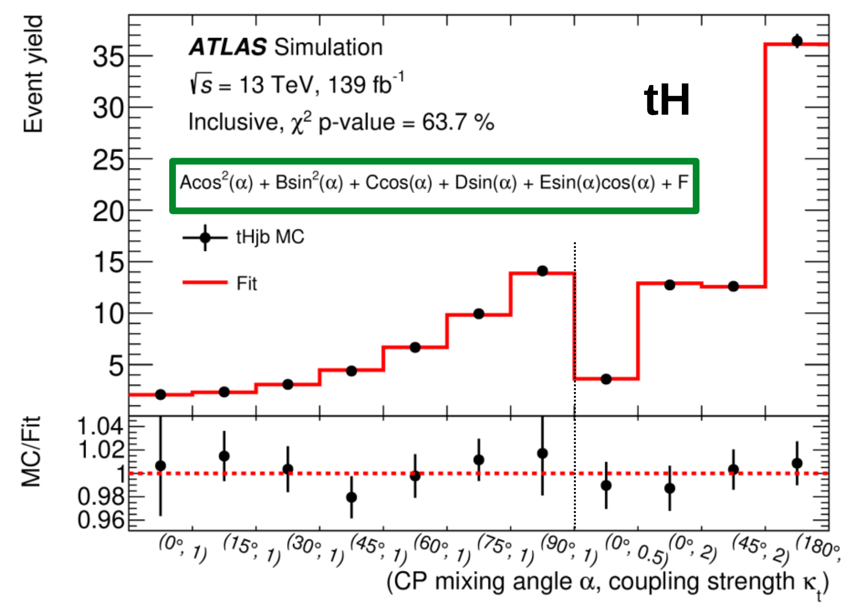

CP properties of the top-Higgs Yukawa coupling (ttH/tH, H→γγ)

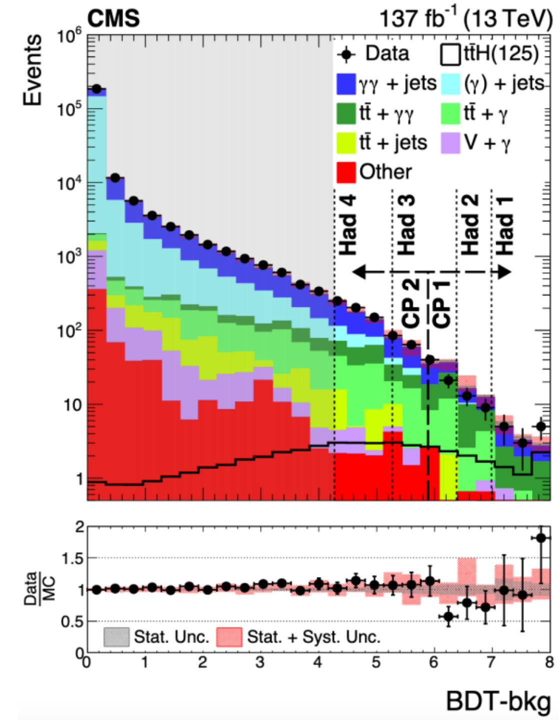

<u>Analysis strategy</u>

Preselection: Hadronic/Leptonic *tt* decays

Several MVAs for object reconstruction (also top quark)

Two event-level MVAs used → define several analysis categories

1: ttH vs. continuum bkg.

2: ttH(/tH) CP-odd vs. CP-even

Signal extraction: fit $m_{\gamma\gamma}$ in all categories

<u>Results:</u> overall, quite similar; limited by data statistics

μ(ttH)~1.4 and **a pure CP-odd coupling excluded at 3.9σ/3.2σ**

tH rate < 12 x σ_{SM} at 95% CL

|α|< 43º at 95% CL

y_t <0 disfavoured *(see 2D contours)*

$$f_{CP}^{Htt} = \sin^2\alpha$$

$|f_{CP}^{Htt}| < 0.67$ at 95% CL

|α|< 55º at 95% CL

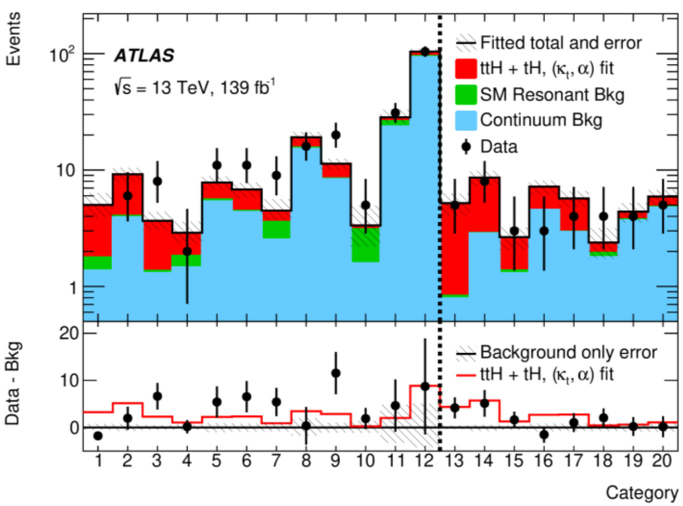

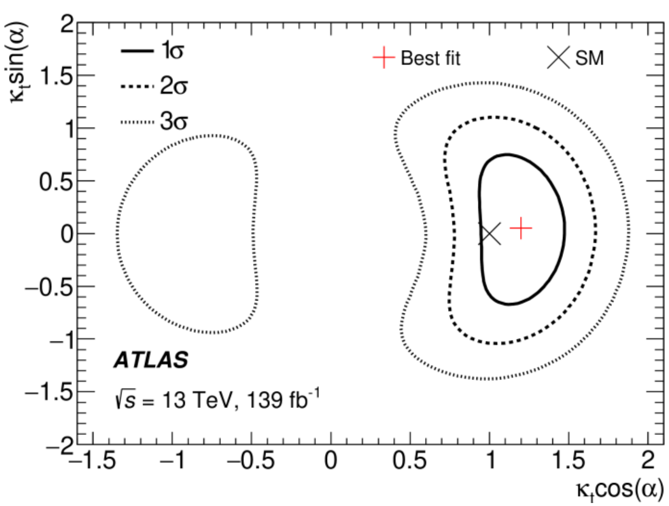

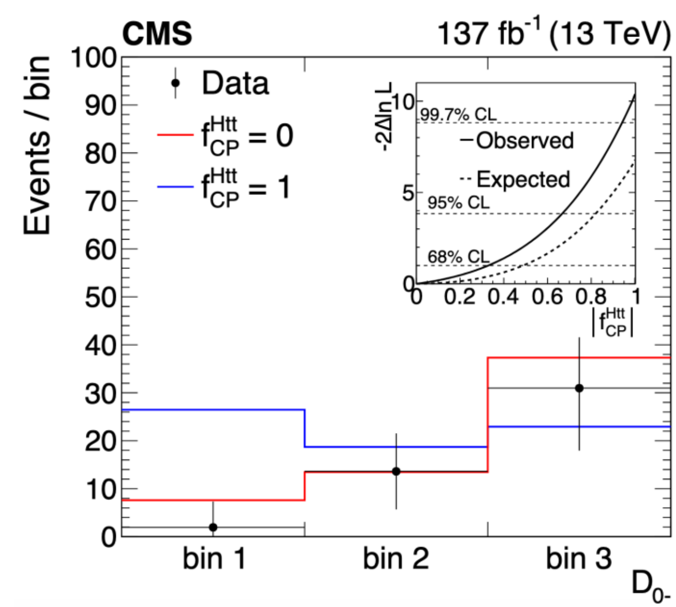

CP properties of the top-Higgs Yukawa coupling (ttH/tH, H→γγ)

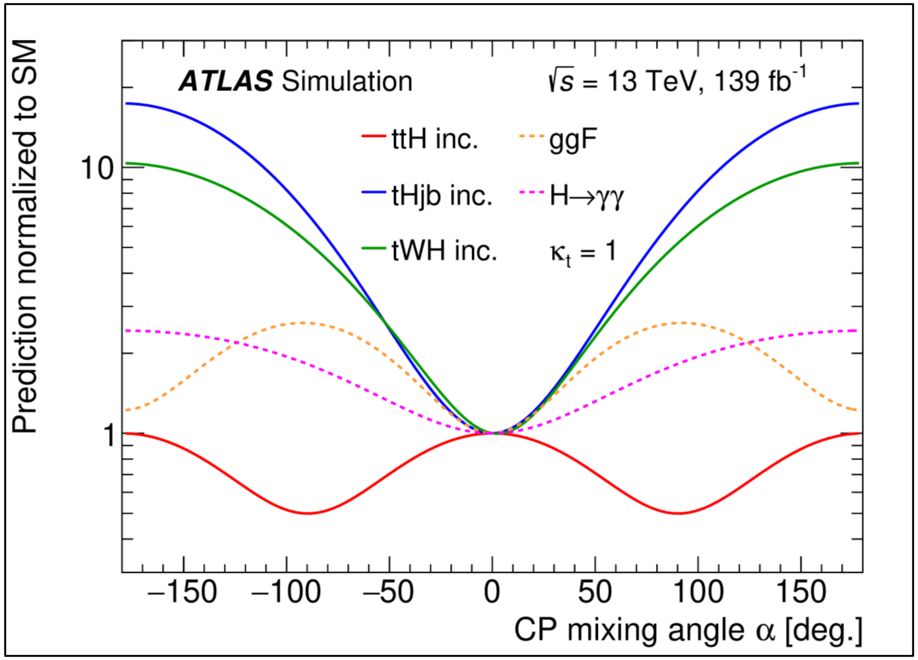

Used in ATLAS

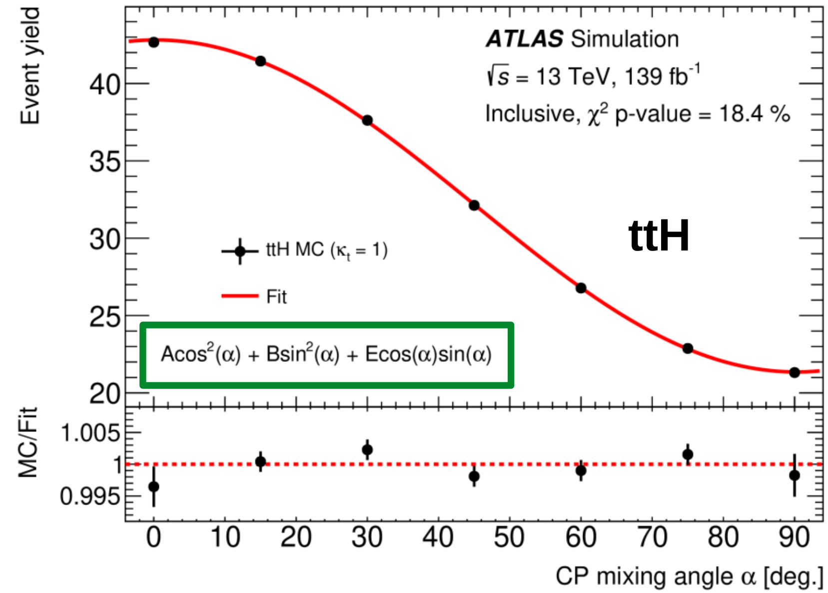

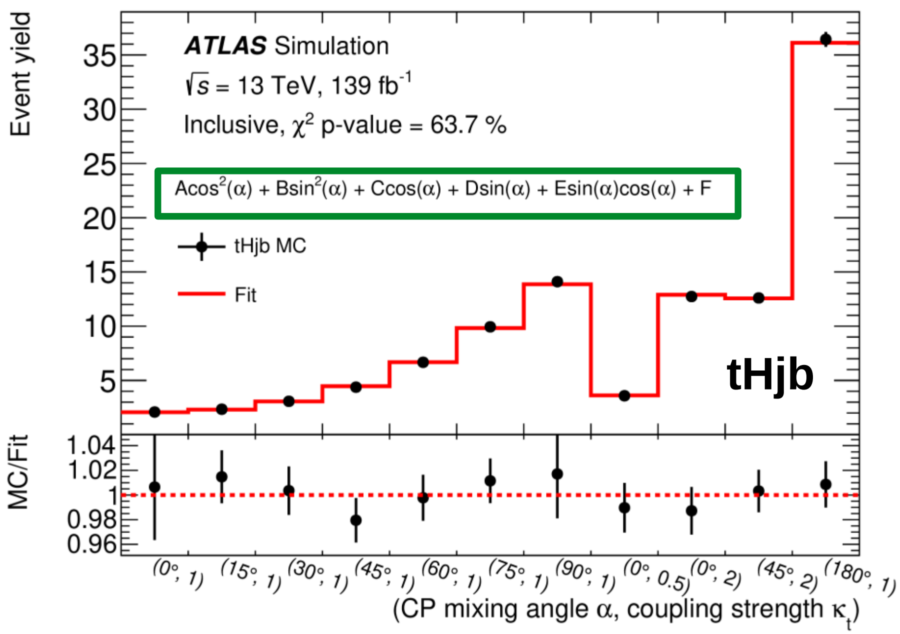

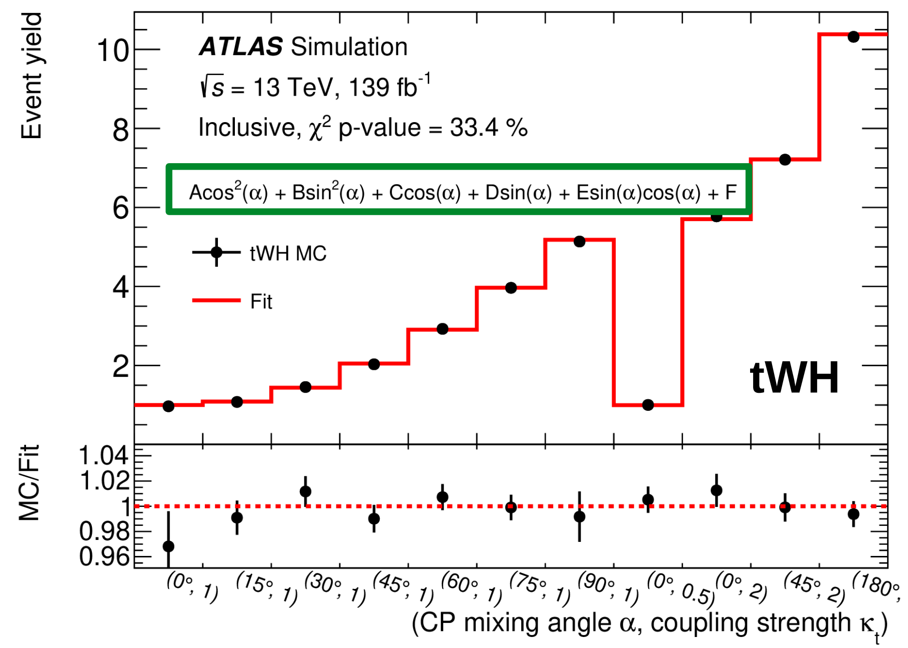

CP properties of the top-Higgs Yukawa coupling (ttH/tH, H→γγ)

arXiv: 2004.04545

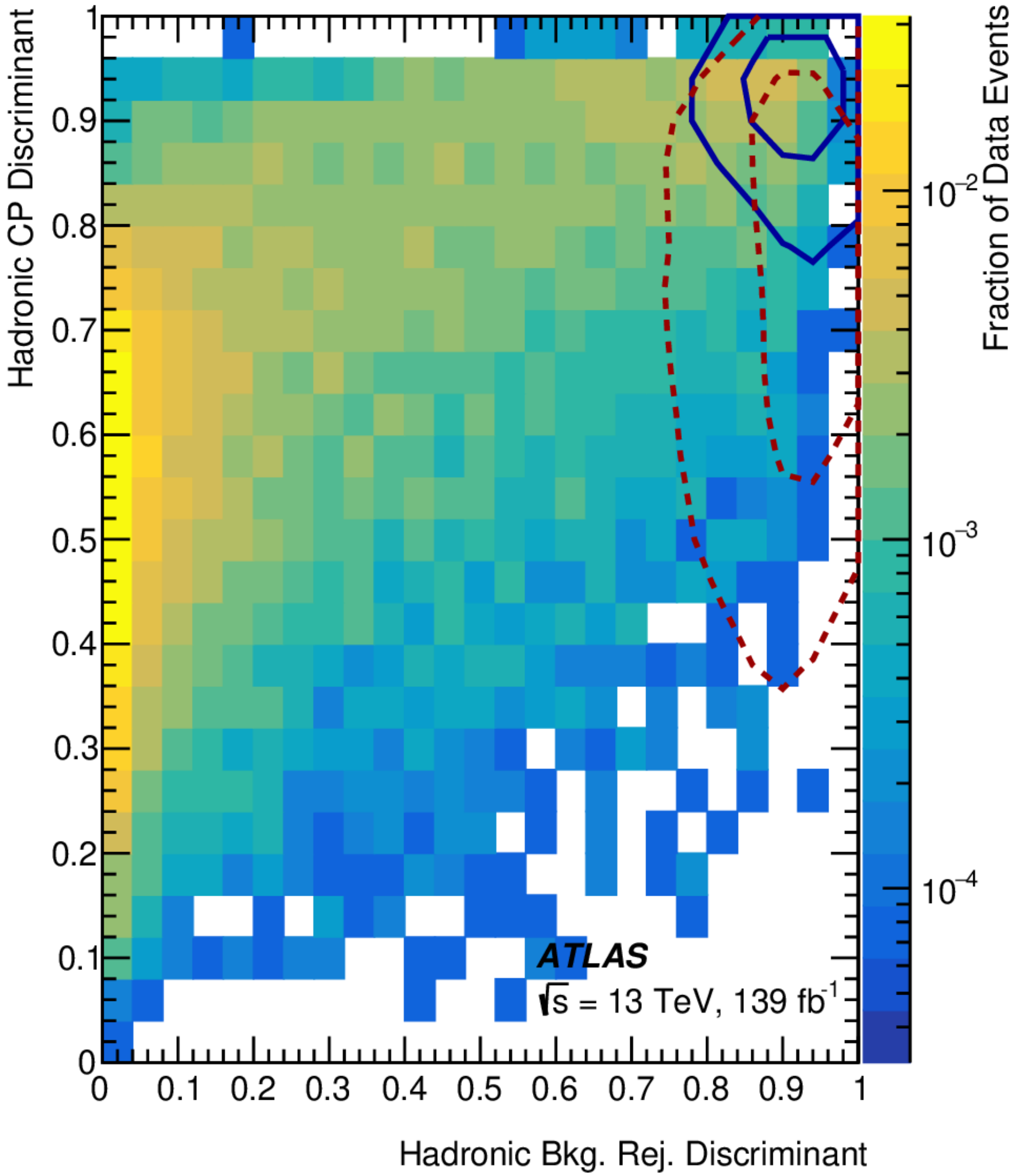

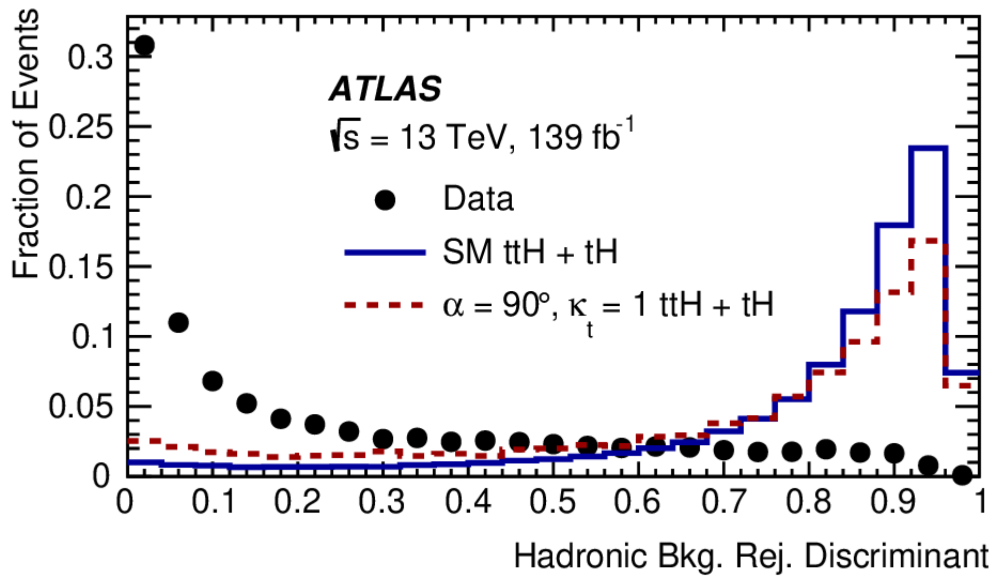

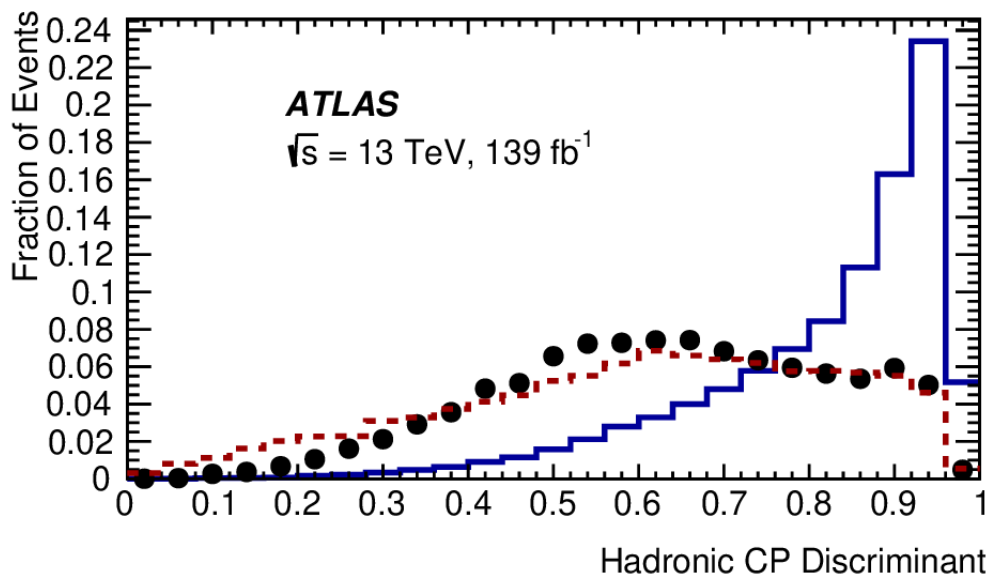

CP properties of the top-Higgs Yukawa coupling (ttH/tH, H→γγ)

(i) $m_{t\bar{t}H}$: invariant mass of the $t\bar{t}H$ system;
(ii) θ_H: angle between the H boson direction and the incoming partons in the $t\bar{t}H$ frame;
(iii) θ_V^*: angle of the $H \to VV(f\bar{f})$ decay with respect to the opposite $t\bar{t}$ direction in the H frame;
(iv) Φ_V^*: angle between the production plane, defined by incoming partons and H, and $H \to VV(f\bar{f})$ decay plane;
(v) θ_t: angle between the top-quark direction and the opposite Higgs direction in the $t\bar{t}$ frame;
(vi) Φ_t^*: angle between the decay planes of the $t\bar{t}$ system and $H \to VV(f\bar{f})$ in the $t\bar{t}H$ frame;
(vii) m_{tt}: invariant mass of the $t\bar{t}$ system;
(viii) θ_W: angle between W^+ and opposite of the $b\bar{b}$ system in the W^+W^- frame;
(ix) Φ_W: angle between the production $(b\bar{b})(W^+W^-)H$ plane and the plane of the W^+W^- system in the $t\bar{t}$ frame;
(x) θ_b: angle between the b quark and opposite of the W^+W^- system in the $b\bar{b}$ frame;
(xi) Φ_b: angle between the planes of the $b\bar{b}$ and W^+W^- systems in the $t\bar{t}$ frame;
(xii) m_{Wb1} or m_{Wb2}: invariant mass of the W^+b or $W^-\bar{b}$ system;
(xiii) θ_{f1} or θ_{f2}: angles between fermion direction and opposite of the b or $\bar{b}$ quark in the W^+ or W^- frame;
(xiv) Φ_{f1} or Φ_{f2}: angle between the W^+ or W^- decay plane and the $\bar{t}W^+b$ or $tW^-\bar{b}$ plane in the t or $\bar{t}$-quark frame;
(xv) $m_{f1\bar{f}1}$ or $m_{f2\bar{f}2}$: invariant mass of the $f_1\bar{f}_1$ or $f_2\bar{f}_2$ system.

Pheno paper PRD94,055023 (2016)

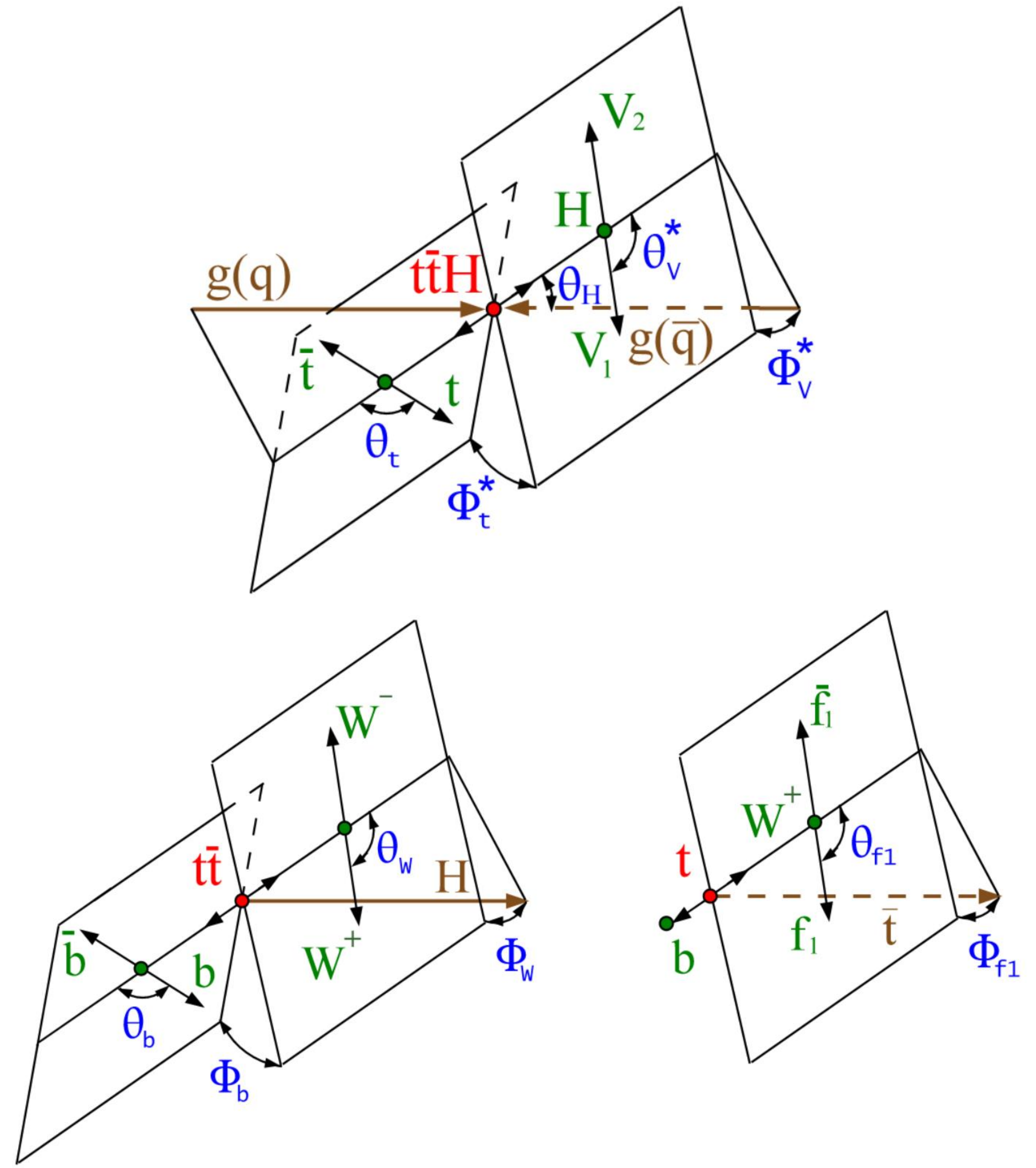

Pheno paper PRD94,055023 (2016)

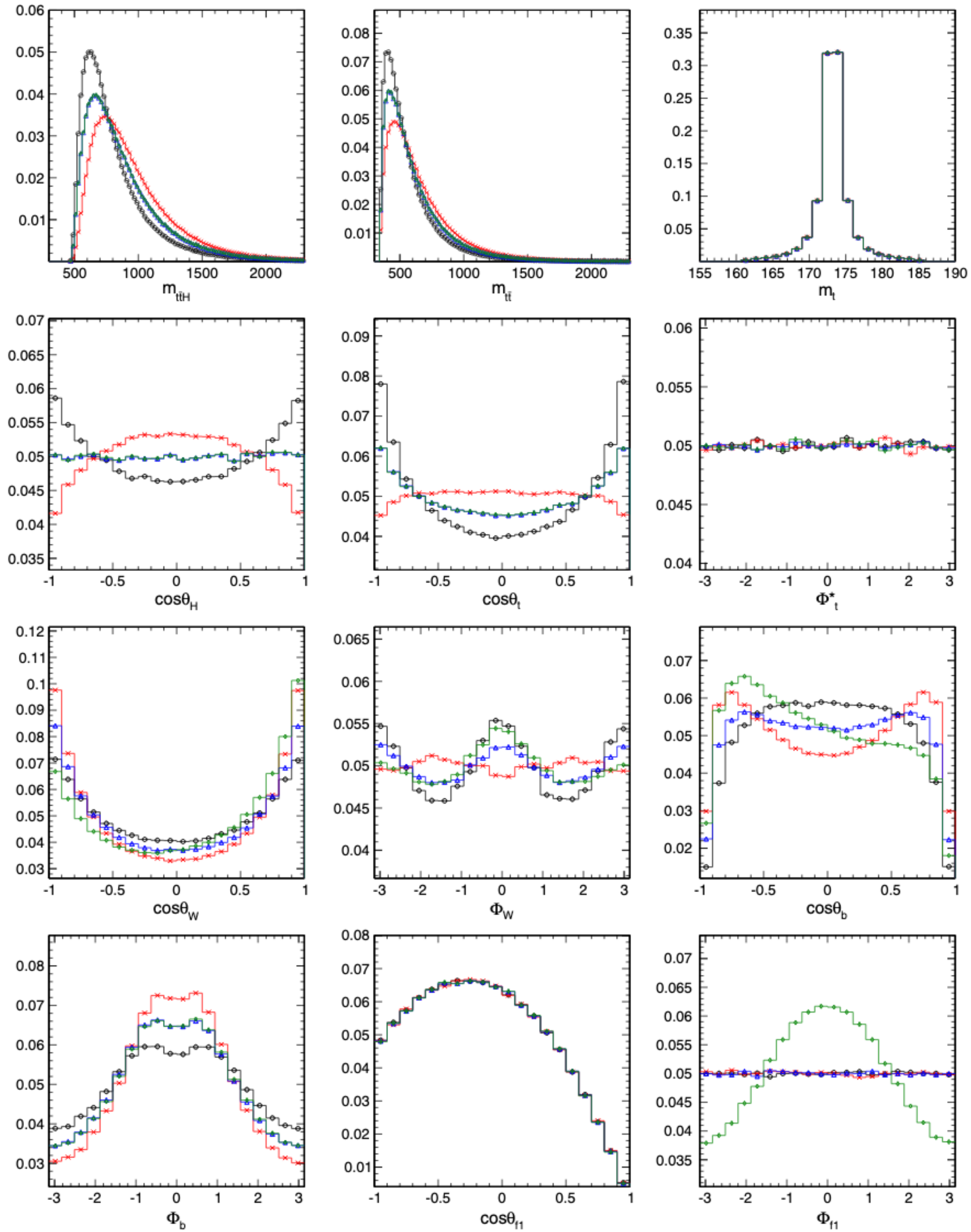

FIG. 5. The normalized angular and mass distributions in the process $pp \to t\bar{t}H$ corresponding to four scenarios of anomalous $t\bar{t}H$ couplings: $f_{CP} = 0$ (SM 0^+, red crosses), $f_{CP} = 1$ (pseudoscalar 0^-, black circles), $f_{CP} = 0.28$ with $\phi_{CP} = 0$ (blue triangles), and $\phi_{CP} = \pi/2$ (green diamonds). The LHC pp energy of 13 TeV and H boson mass of 125 GeV are used in simulation. See the text for the definition of all observables.

CP-even

CP-odd

Mixture with ϕ_{CP}=0º

Mixture with ϕ_{CP}=90º

Pheno paper PRD94,055023 (2016)

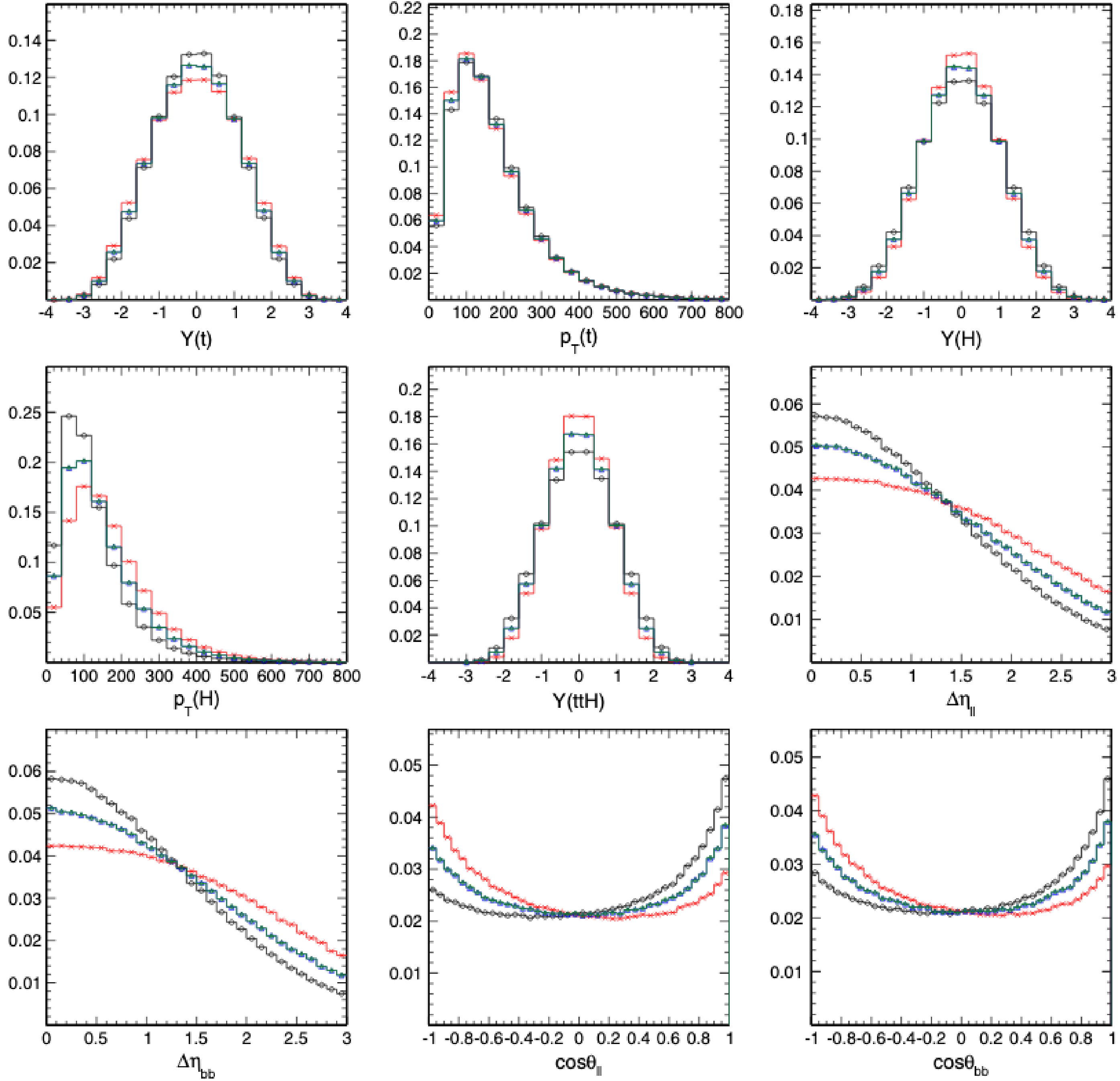

CP-even

CP-odd

Mixture with ϕ_{CP}=0º

Mixture with ϕ_{CP}=90º

FIG. 14. The kinematic distributions in the process gg and $q\bar{q} \to t\bar{t}H$ defined in the laboratory frame: top-quark rapidity $[Y(t)]$, transverse momentum of the top quark $[p_T(t)]$, H boson rapidity $[Y(t)]$, transverse momentum of the H boson $[p_H(t)]$, $t\bar{t}H$ system rapidity $[Y(t\bar{t}H)]$, pseudorapidity difference between the two down-type fermions decayed from top and antitop $(\Delta\eta_{ll})$ and between two bottom quarks $(\Delta\eta_{bb})$, $\cos\theta_{ll}$ between the two down-type fermions, and $\cos\theta_{bb}$ between the two bottom quarks. Four scenarios of anomalous $t\bar{t}H$ couplings are shown: $f_{CP} = 0$ (SM 0^+, black circles), $f_{CP} = 1$ (pseudoscalar 0^-, red crosses), $f_{CP} = 0.28$ with $\phi_{CP} = 0$ (blue triangles), and $\phi_{CP} = \pi/2$ (green diamonds). The LHC pp energy of 13 TeV and H boson mass of 125 GeV are used in simulation.

CP properties of the top-Higgs Yukawa coupling (ttH/tH, H→γγ)

Pheno paper PRD94,055023 (2016)

$$f_{CP} = \frac{|\tilde{\kappa}_f|^2}{|\kappa_f|^2 + |\tilde{\kappa}_f|^2}, \qquad \phi_{CP} = \arg(\tilde{\kappa}_f/\kappa_f),$$

$$= \sin^2\alpha \qquad\qquad = 0 \text{ or } \pi.$$

$$\mathcal{P}_{\text{sig}}(\vec{x}_i; f_{CP}, \phi_{CP}) = (1 - f_{CP})\mathcal{P}_{0^+}(\vec{x}_i) + f_{CP}\mathcal{P}_{0^-}(\vec{x}_i) + \sqrt{f_{CP}(1 - f_{CP})}(\mathcal{P}_{\text{int}}(\vec{x}_i)\cos\phi_{CP} + \mathcal{P}^{\perp}_{\text{int}}(\vec{x}_i)\sin\phi_{CP}),$$

$$\mathcal{D}_{0-} = \frac{\mathcal{P}_{0^+}(\vec{\Omega})}{\mathcal{P}_{0^+}(\vec{\Omega}) + \mathcal{P}_{0^-}(\vec{\Omega})}$$

$$\mathcal{D}_{CP} = \frac{\mathcal{P}_{\text{int}}(\vec{\Omega})}{\mathcal{P}_{0^+}(\vec{\Omega}) + \mathcal{P}_{0^-}(\vec{\Omega})}$$

$$\mathcal{D}^{\perp}_{CP} = \frac{\mathcal{P}^{\perp}_{\text{int}}(\vec{\Omega})}{\mathcal{P}_{0^+}(\vec{\Omega}) + \mathcal{P}_{0^-}(\vec{\Omega})}$$

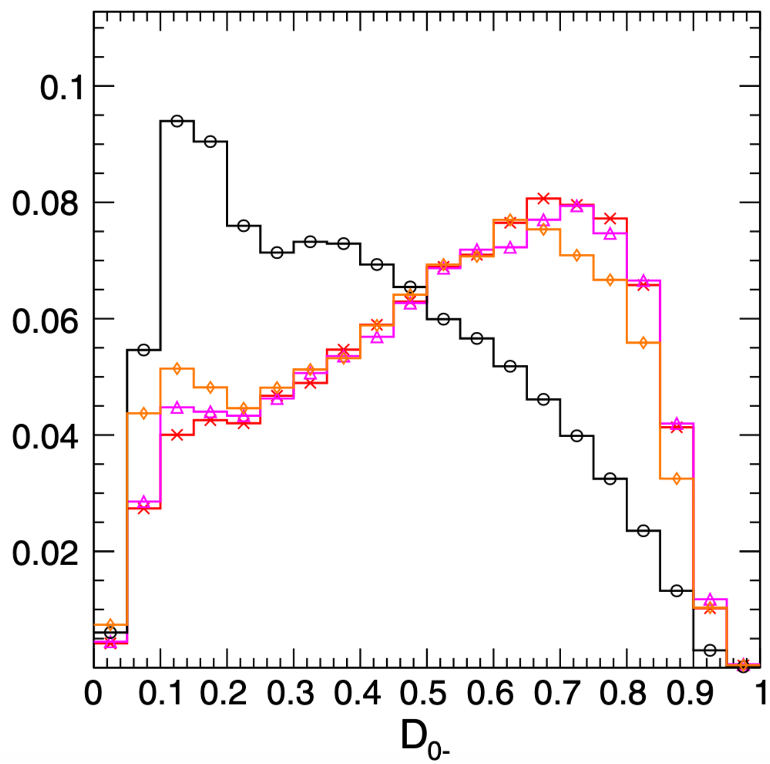

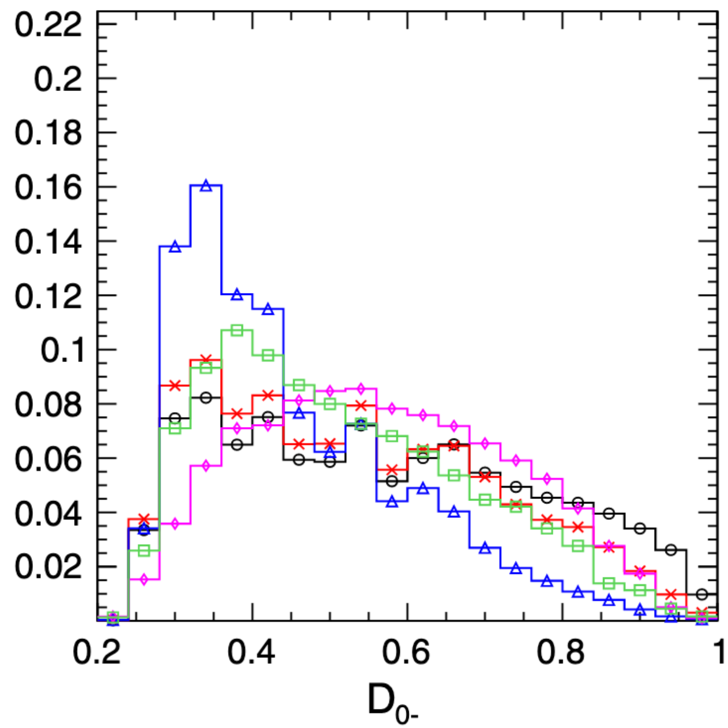

Only D_{0-} discriminant is used in CMS analysis (using a BDT instead of using MEM)

D_{CP} requires flavor of tt decay particles, not possible in full hadronic and semi-leptonic, dropped in this analysis

Hff-induced ttH CP-odd (red, magenta)
Hff-induced ttH CP-even (black)
ttγγ background (orange)

Hff-induced tH CP-odd (red)
Hff-induced tH CP-even (blue)
HVV-induced tH considered background (black)